MILLIMETER WAVE TRANSITIONS FOR FREQUENCY CONTROL

SURFACE IONIZATION OF LITHIUM FLUORIDE AND THALLIUM ON TUNGSTEN, RHENIUM, AND PLATINUM SURFACES

SPECIAL TECHNICAL PROGRESS REPORT NO. 1

March, 1963

Contract No. DA-36-039 SC-87277

Placed by: U. S. Army Signal Supply Agency
Fort Monmouth Procurement Office
Fort Monmouth, New Jersey

Department of the Army Project No. 3A99-15-001

Submitted by:

Assistant Professor Svein G. Andresen

University of Colorado
Boulder, Colorado

MILLIMETER WAVE TRANSITIONS
FOR FREQUENCY CONTROL

SURFACE IONIZATION OF LITHIUM FLUORIDE AND THALLIUM ON TUNGSTEN, RHENIUM, AND PLATINUM SURFACES

SPECIAL TECHNICAL PROGRESS REPORT NO. 1

March, 1963

Contract No. DA-36-039 SC-87277

Placed by: U. S. Army Signal Supply Agency
Fort Monmouth Procurement Office
Fort Monmouth, New Jersey

Department of the Army Project No. 3A99-15-001

Submitted by:

Assistant Professor Svein G. Andresen

University of Colorado
Boulder, Colorado

ABSTRACT

Ionization efficiencies of lithium, lithium fluoride, and thallium on hot tungsten, rhenium and platinum surfaces were studied using molecular beam technique. The temperature dependence of the efficiencies as well as aging effects of the filaments used were determined. Careful design of the apparatus allowed pressures of the order of 5×10^{-9} mm Hg to be maintained at the detector contributing to the degree of cleanliness of the hot surfaces.

As a by-product of the efficiency measurements, vapor pressure data, and estimated molecular scattering cross sections for LiF, Li, and Tℓ were obtained. Signal-to-noise ratios were estimated from the recordings made. An anomalous effect was discovered in the case of LiF ionizing on platinum similar to that discovered by other workers for KF on platinum. The much higher degree of ionization obtained for LiF as compared to Li is ascribed to the presence of an adsorbed layer of fluorine yielding effects similar to that on an oxidized filament.

TABLE OF CONTENTS

LIST OF FIGURES

SECTION 1

INTRODUCTION

The following study of the surface ionization properties of lithium fluoride and thallium was undertaken due to the recent interest in these molecules for use in beam frequency standards. Here at the University of Colorado, we are presently investigating molecular transitions in the region above 100 kMc/s to see if it is feasible to develop a frequency standard which can be expected to have a greater precision than the cesium beam machines currently in use. The project is divided into two parts. The first of these is a survey of various molecules to see which, if any, have the necessary physical properties for an improved frequency standard; the second is a survey of various possible detectors and a consideration of possible improvements in them which could be made for detecting the particular molecule which proves to have the other interesting properties. This paper deals with part of the second problem; i.e., the measurement of surface ionization efficiency, its dependence upon the type of filament used, temperature of the filament, and aging effects. More specifically, we have investigated lithium fluoride, lithium,

and thallium ionizing on tungsten wires, tungsten wires drawn from a single tungsten crystal, rhenium wires, and platinum wires.

Surface ionization means the formation of positive or negative ions on the surface of a hot metal. The ions of interest are usually those due to a beam of neutral atoms or molecules impinging on the hot metal. Ions may also be produced by the impurities contained in the metal itself, or by the background molecules of the atmosphere of the vacuum system. By a suitable arrangement of an electric field and a collecting plate near the hot metal surface, some or all of the ions evaporated may be made to strike the collector so as to cause a current in an external circuit. In this manner it is possible to detect the presence of a beam of neutral atoms or molecules.

Many of the basic laws of surface ionization are not well understood. The so-called Saha-Langmuir law of surface ionization apparently works well for the alkali metals evaporating from a tungsten surface. The reason is that the efficiency of the process is so high that the true Saha-Langmuir type of ionization tends to swamp out any other competing mechanism. Various deviations from this law have been attributed to such things as non-homogeneity of the crystalline surfaces, adsorbed layers of oxygen, various reflection coefficients, etc.[7,8,9]

In the present work we find that many of the deviations may be explained by the effect on the surface ionization parameters by an adsorbed layer consisting of various types of molecules or atoms.

The adsorbed layer may arise as a consequence of impurities present in the filaments, in the vacuum system's atmosphere, or a layer may form from the beam species itself.

SECTION 2

THEORETICAL CONSIDERATIONS

Surface ionization was first observed in 1923 by K. H. Kingdom, I. Langmuir,[1] and H. E. Ives,[2] with the formation of positive ions. The possibility of obtaining negative ions with surface ionization was first proposed by Morgulis[3] in 1934. Negative ion formation was first observed by P. P. Sutton and J. E. Mayer[4] in 1935.

The quantitative parameters for surface ionization are first the degree of ionization

$$\alpha = \frac{n_+}{n_a}, \tag{2-1}$$

and the ionization efficiency

$$\eta_i = \frac{n_+}{n_i}, \tag{2-2}$$

where

n_i = atomic flux reaching unit area of the surface per unit time (no. of incident atoms),

n_+ = positive ion flux evaporating from unit area

per unit time,

n_a = atomic flux evaporating from unit area per unit time.

In the steady state,

$$n_i = n_+ + n_a, \tag{2-3}$$

so that α and η_i are related by

$$\eta_i = \frac{\alpha}{1 + \alpha}, \tag{2-4}$$

$$\alpha = \frac{\eta_i}{1 - \eta_i}. \tag{2-5}$$

In general, α is a function of the work function ϕ and temperature T of the surface, of the ionization potential I of the atoms, and of the electric field intensity E at the surface.

Langmuir and Kingdom derived an expression for α thermodynamically assuming E to be zero.[5] This theory has as its basis the work of Saha,[6] which relates the concentrations of ions, atoms, and electrons in a gas on the surface of a metal in thermodynamic equilibrium. Using a statistical expression for the equilibrium constant and assuming that the concentration of the electronic gas is determined by the thermionic emission of electrons from

the metal, Langmuir and Kingdom found that

$$\frac{n_+}{n_a} = \frac{w_+}{w_a} \exp\left[\frac{e(\phi - I)}{kT}\right], \qquad (2\text{-}6)$$

where

$\frac{w_+}{w_a}$ = ratio of statistical weights, and is equal to 1/2 for alkali metals,

e = charge on an electron,

ϕ = work function of the surface,

I = ionization potential of the atom.

Equation (2-6) is usually called the Saha-Langmuir equation. (See appendix). M. J. Copley and T. E. Phipps,[7,8] and S. Datz and E. H. Taylor[9] studied the possibility of reflections of ions and atoms from a surface and derived the following expression for the ratio of the number of ions to atoms evaporating from a homogeneous surface:

$$\frac{n_+}{n_a} = \frac{1 - r_+}{1 - r_a} \quad \frac{w_+}{w_a} \exp\left[\frac{e(\phi - I)}{kT}\right], \qquad (2\text{-}7)$$

where

r_a = reflection coefficient for atoms,

r_+ = reflection coefficient for ions.

The degree of ionization, or the ionization efficiency, is given by Eq. (2-5). Combining Eqs. (2-5) and (2-7), and

assuming that part of the incident beam is reflected with a reflection coefficient r_i, we obtain

$$\eta_i = \frac{n_+}{n_i}$$

$$= (1 - r_i)\left[1 + \frac{w_a}{w_+}\frac{1 - r_a}{1 - r_+}\exp\left\{-\frac{e(\phi - I)}{kT}\right\}\right]^{-1}. \tag{2-8}$$

Equation (2-8) is plotted in Fig. 1 with the factor

$$\frac{w_a}{w_+}\frac{1 - r_a}{1 - r_+} = 1, \text{ and } r_i = 0; \text{ i.e.,} \tag{2-8a}$$

$$\eta_i = \frac{n_+}{n_i} = \frac{1}{1 + \exp\frac{e(I - \phi)}{kT}}.$$

The effect of a non-zero value of r_i is simply to change the scale on the ordinate in such a manner as to make the upper "asymptote" labeled 100% intersect the ordinate at $1 - r_i$ instead of 1. Similarly, the factor $\frac{w_a(1 - r_a)}{w_+(1 - r_+)}$ changes the position of the $I - \phi = 0$ asymptote either up or down about the 0.5 value on the ordinate depending on its numerical value.

L. N. Dobretsov[10] studied the modification necessary in the ion emission equation to account for the presence of an electric field at the metal surface. The thermodynamic disturbance set up by this field results in a

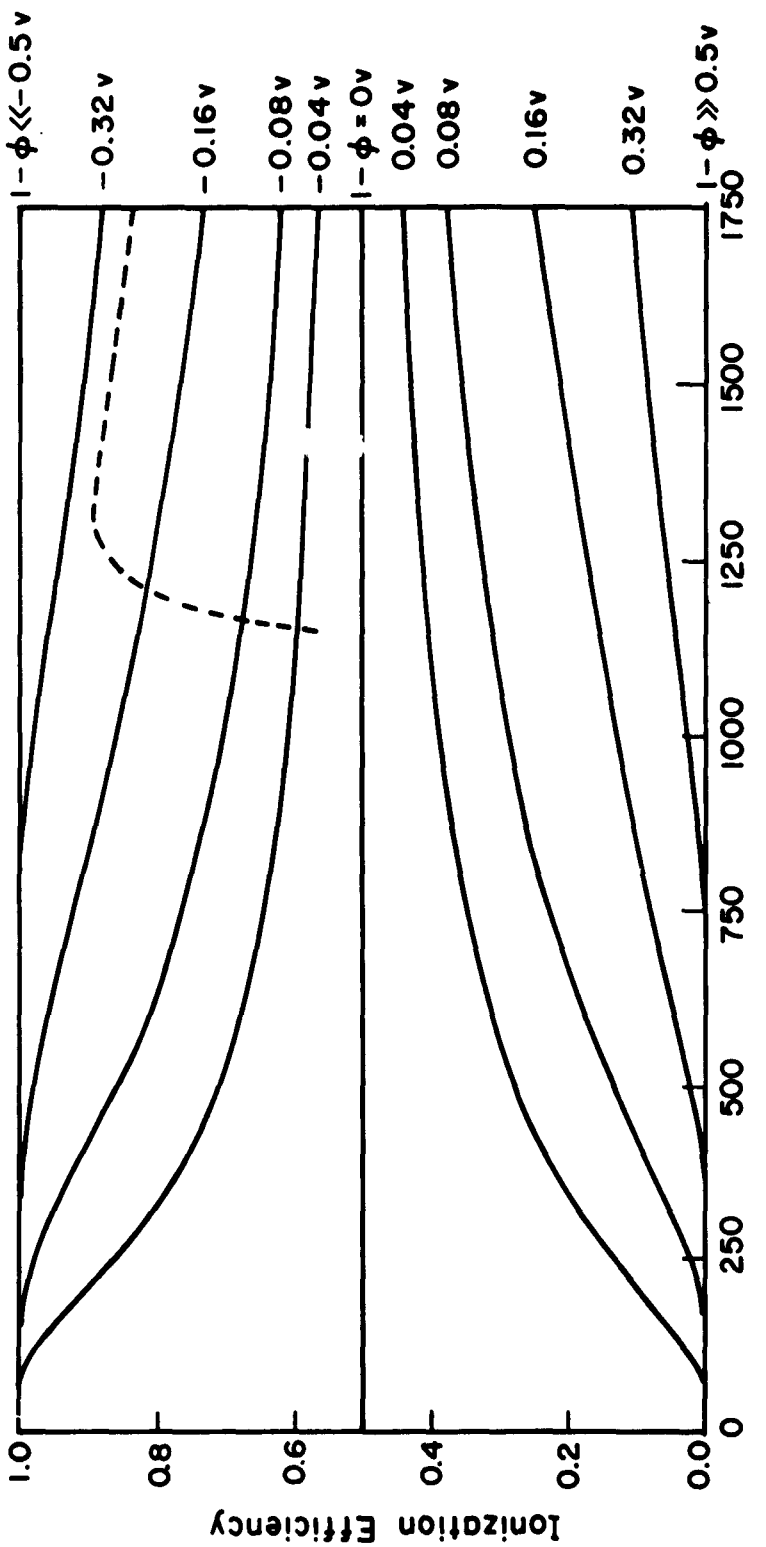

IONIZATION EFFICIENCY VS. FILAMENT TEMPERATURE (THEORETICAL)
PARAMETER BEING $1-\phi$

DOTTED CURVE FOR POTASSIUM FLUORIDE ON TUNGSTEN (EXPERIMENTAL)

Figure 1

modification similar to the Schottky modification of the Richardson-Dushman equations for the thermionic emission of electrons in the presence of an electric field. Equation (2-7) becomes

$$\frac{n_+}{n_a} = \frac{1 - r_+}{1 - r_a} \frac{w_+}{w_a} \exp \frac{e}{kT} \left\{ \phi - I + Ex_o + \sqrt{\frac{eE}{4\pi\epsilon_o}} + \frac{E^2}{2e}\left(A_a - A_+\right) \right\}, \tag{2-9}$$

where

E = electric field intensity,

ϵ_o = permittivity of free space,

A_+ = polarizability of the ion,

A_a = polarizability of the atom,

x_o = distance from the surface at which the electric field compensates for the image force field.

Furthermore, a second correction to Eq. (2-7) may be necessary in the presence of an electric field. Consider the enhancement of thermionic emission from certain metals by the application of an external field, known as the Schottky effect. This effect is explained as being due

to a lowering (by the applied field) of the effective potential barrier close to a metal surface. The theory predicts a linear relationship between the logarithm of the emitted current and the square root of the electric field intensity. Experimental work by Seifert, Turnbull, and Phipps[19,20] showed that the relationship is not quite linear but that there exist periodic deviations from the Schottky line. This effect was recognized to be quantum mechanical in nature and due to reflections of electrons having energies higher than the potential barrier maximum. In the case of surface ionization a similar effect may be in operation.

Equation (2-9) may be simplified by considering in the exponent the relative magnitudes encountered in practice. x_o is estimated to be of the order of the adsorbed atom radius, and $(A_o - A_+) \cong 10^{-40}$ farad-m^2. Then, if we assume that E is less than 10^8 volts/meter, the terms Ex_o and $\frac{E^2}{2e}(A_o - A_+)$ may be neglected in comparison to the term $\sqrt{\frac{eE}{4\pi\epsilon_o}}$. Thus,

$$\frac{n_+}{n_a} = \frac{1 - r_+}{1 - r_a}\frac{w_+}{w_a} \exp\left[\phi - I + \sqrt{\frac{eE}{4\pi\epsilon_o}}\right]. \qquad (2\text{-}10)$$

Furthermore, the last term in the exponent of (2-10) takes on significance only if the difference $\phi - I$ is small. For example, the numerical value of $\sqrt{\frac{eE}{4\pi\epsilon_o}}$ is about

$3.8 \times 10^{-5} \sqrt{E}$. Therefore, for $E = 10^6$ volts/m or 10^3 volts/mm, which is close to a practical maximum value, the apparent increase in the work function is only 0.038 volts. This small increase may be important if $(\phi - I)$ is small.

The Saha-Langmuir equation above assumes that the degree of adsorptive coating of the surface by atoms of the element being ionized is small at all filament temperatures. Thus, as shown in Fig. 1 if $(I - \phi) < 0$, the largest ion current will be observed when $T = 0$. When $(I - \phi) > 0$, the ion current is zero at zero temperature and increases with an increase in T. Under real experimental conditions it is found that as T is decreased there is a sudden drop-off in the ion current for the case $(I - \phi) < 0$ as indicated by the dotted curve in Fig. 1, which is for KF on tungsten as obtained by Datz and Taylor[16] and is typical for most experiments following the Saha-Langmuir equation for ionization in the high temperature region.

The apparent reason for this behavior was pointed out by Zandberg and Ionov[12] to be due to an adsorbed layer of ionized atoms of the element being ionized. The work function of the surface is consequently modified and the foregoing equations cannot be used below the threshold temperature.

The concentration N of adsorbed atoms on the surface at temperature T is related to the atomic flux η_i in the steady state by[12]

$$\eta_i = N\left[A \exp\left(-\frac{\ell_+}{kT}\right)+B \exp\left(-\frac{\ell_i}{kT}\right)\right], \qquad (2\text{-}11)$$

where A and B are coefficients which depend slightly on the temperature, ℓ_+ and ℓ_i are the isothermal heats of evaporation in the presence of an electric field at the surface. Thus,

$$N = f(\eta_i,\ \ell_+,\ \ell_i,\ E,\ T). \qquad (2\text{-}12)$$

As pointed out by Zandberg and Ionov, this leads to a maximum of the ion current versus temperature curve for the case $(I - \phi) < 0$. Furthermore, for this case they show that for constant ion current and atomic flux, η_i, the threshold temperature decreases linearly with an increase in $\sqrt{E}$. For the other case, $(I - \phi) > 0$, an increase in N induces a steeper current drop than would follow from the Saha-Langmuir equation.

A metal surface with an identical work function at all points could only be provided by the face of a perfect single crystal with no adsorbed impurity atoms. The surface of ordinary drawn metal wires on which surface

ionization is usually investigated are mosaics of different crystalline faces with different closeness of atomic packing and correspondingly different work functions. On such surfaces ionization cannot be represented by (2-6), (2-7), (2-8), (2-9), or (2-10). It has been shown by Dobretsov[10] that electrons are emitted mostly from surfaces having low work functions, and ions from regions having high work functions.

J. Zemel[11] has shown that ionization from a patchy surface which can be described as a sum of surfaces with areas A_k, and work function ϕ_k, may be expressed as

$$\frac{n_+}{n_a} = \left[\sum_k \left(\frac{A_k}{1 + \frac{w_a}{w_+} \frac{1 - r_a}{1 - r_+} \exp \frac{e(I - \phi)}{kT}} \right) - 1 \right]^{-1} . \tag{2-13}$$

E.Y. Zandberg and N. I. Ionov[12] consider the modification of (2-13) on a patchy surface in the presence of an electric field and obtained the ion current from the surface:

$$I_+ = \sum_k \frac{e\, A_k\, \eta_i \frac{w_+}{w_a}}{\frac{w_+}{w_a} + \exp \frac{e}{kT} (I - \phi_k - \psi)} , \tag{2-14}$$

where:

ψ = apparent increase in work function of each patch due to the applied electric field, and

η_i = number of incident atoms per unit time per unit area.

Zandberg and Ionov divide the surface under consideration into two groups. The group for which

$$e(I - \phi_k - \psi) > kT$$

is valid, is denoted by m, while all other patches are denoted by i. They then show that the total ion current may be given by

$$I_+ = e \frac{w_+}{w_a} \eta_i \left[\sum_m A_m \exp \frac{e}{kT} (\phi_m + \psi - I) + \sum_i \frac{A_i}{\frac{w_+}{w_a} + \exp \frac{e}{kT} (I - \phi_i - \psi)} \right]. \quad (2\text{-}15)$$

It is felt that the various theories describe only one of several mechanisms responsible for surface ionization and that some light may be thrown on this problem by using better experimental techniques, especially in the field of ultra-high vacuum technique.

SECTION 3

EXPERIMENTAL APPARATUS

Figure 2 shows a schematic diagram of the molecular beam machine used for testing various detectors and beam molecules. The left-hand chamber is the oven or source chamber; the middle chamber contains a beam defining slit which is adjustable both in width and horizontal position; and the right-hand chamber contains the detector.

Figure 3 shows a photograph of the beam machine. Figure 4 shows a close-up of the oven chamber including a liquid nitrogen cold trap. This chamber is pumped by an oil diffusion pump. The oven is mounted on a square plate which floats on a rubber 0-ring on top of the circular flange of the oven chamber. Micrometer screws are used to position the oven and align the beam with the detector. An ion gauge is connected to the oven chamber. There are also electrical feedthroughs and an observation port. The purpose of the observation port is to be able to check the source slit in the oven for possible clogging. The oven chamber is manufactured from stainless steel 304, all seams are welded, and rubber 0-rings are used to seal

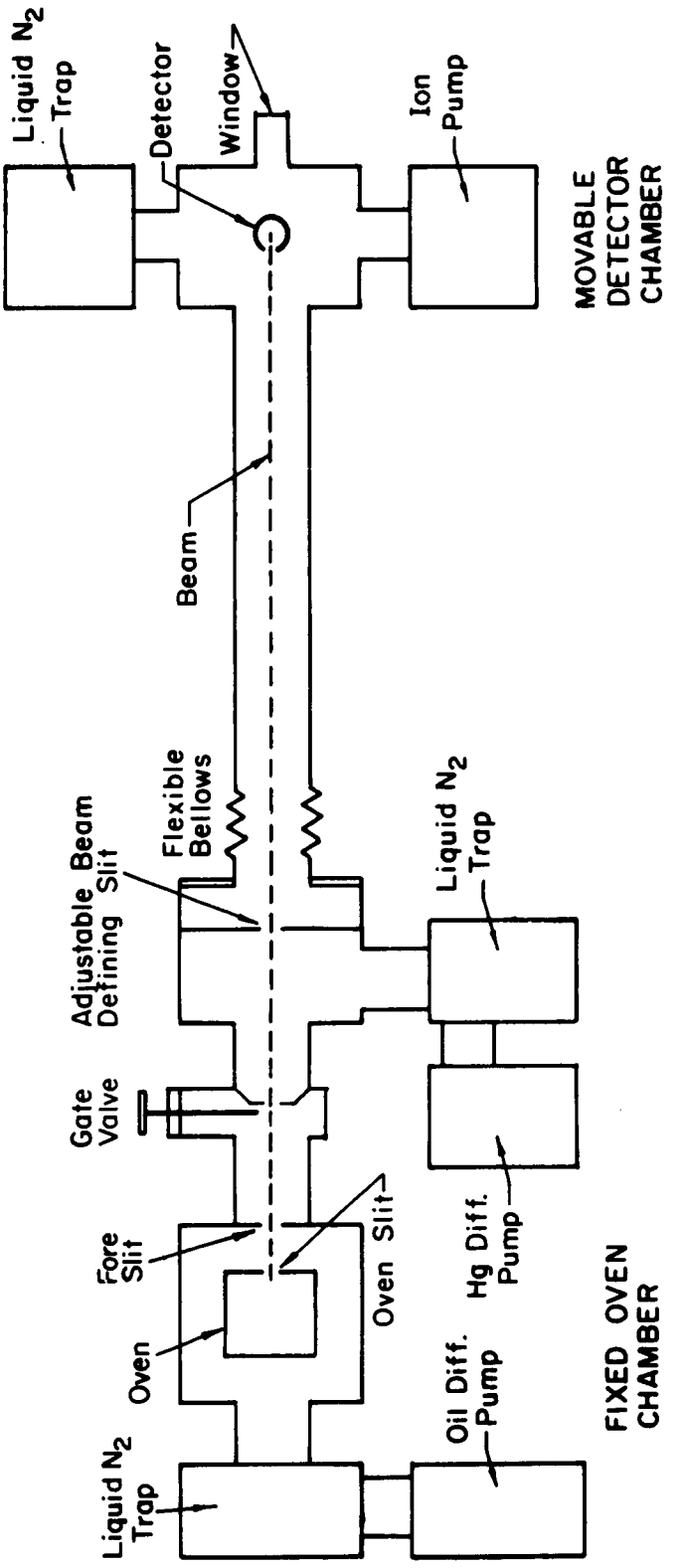

SCHEMATIC ARRANGEMENT OF MOLECULAR BEAM MACHINE

Figure 2

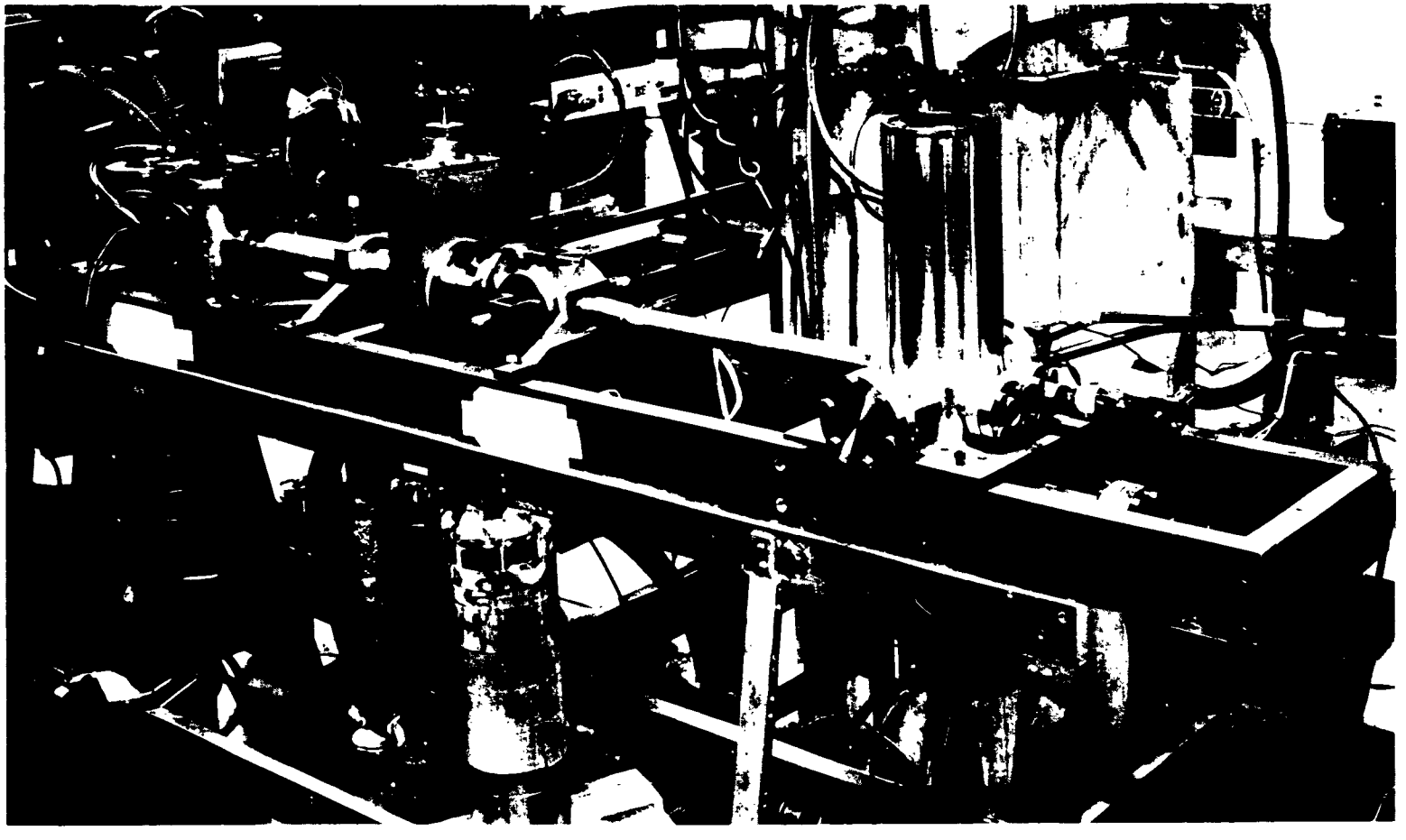

EXPERIMENTAL BEAM MACHINE

Figure 3

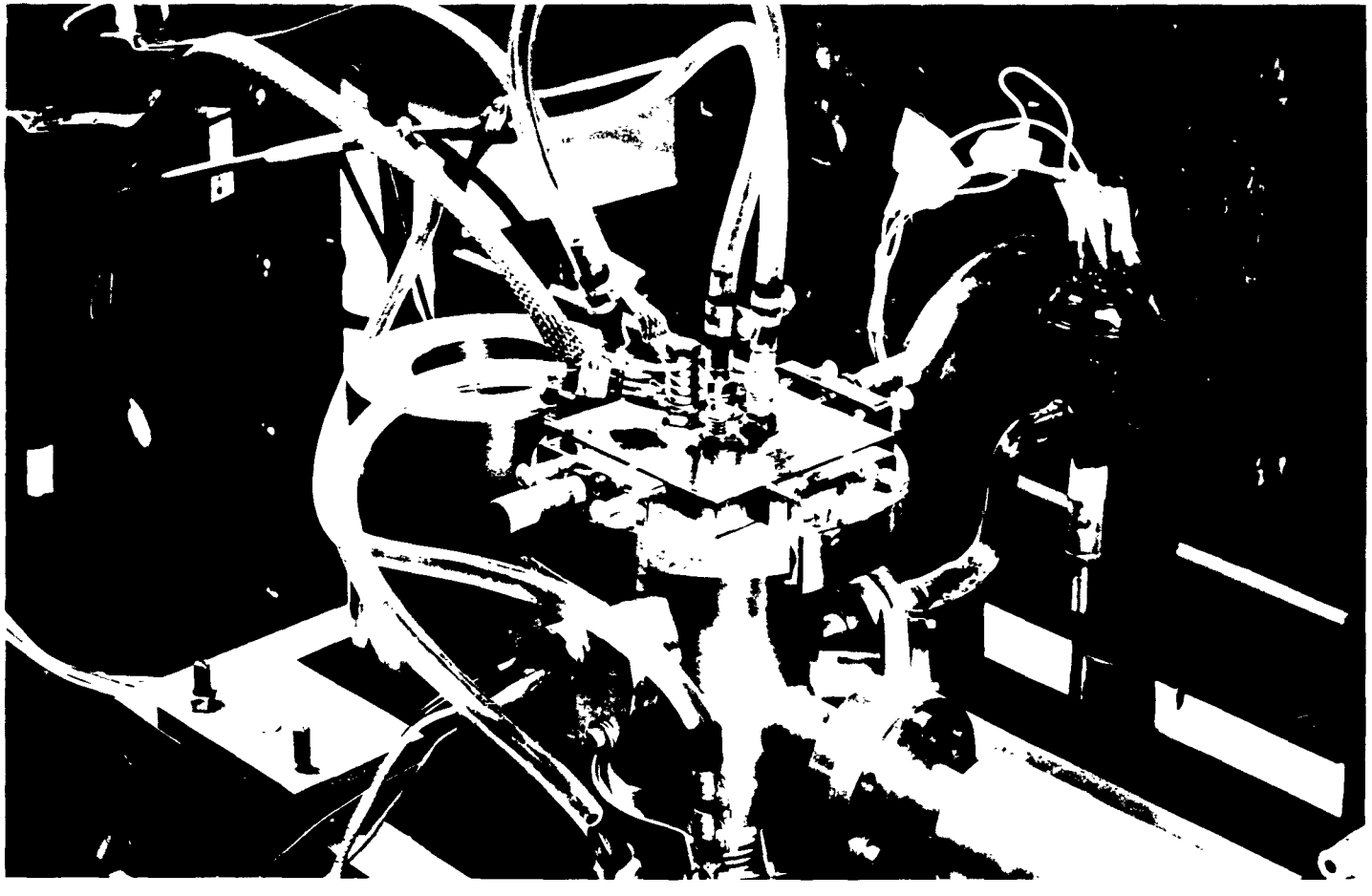

OVEN CHAMBER

Figure 4

all flanges. The operating pressure in this part of the system was found to be 2 x 10^{-6} mm Hg with the oven at about 800°C.

The source or oven is manufactured from a tube of stainless steel 304, 5/16" in diameter. It is approximately 2.5 inches long and contains a slit 0.005" by 10 mm near the top. It is supported by two ceramic rods 1/8" in diameter and is heated by radiation from a helical molybdenum heater. The whole assembly is surrounded by two heat shields, one of bright molybdenum, the other a water-cooled copper cylinder, (see Fig. 5). To maintain the oven at 800°C requires about 200 watts of power.

The middle chamber, or drift space, is pumped by a mercury diffusion pump and a liquid nitrogen cold trap. The operating pressure is approximately 5 x 10^{-7} mm Hg. This chamber contains the beam defining slit whose position and width may be varied by the external micrometer screws. The beam defining slit also serves the purpose of a very effective baffle between the relatively low vacuum of the drift space and the high vacuum of the detector chamber. Further baffling action is obtained by the tubulation (1" diameter) between chambers. Between the drift space and the source chamber is a high-vacuum gate valve which allows the detector and drift space vacuum to be maintained while changing the source material. It also provides for the interruption of the beam.

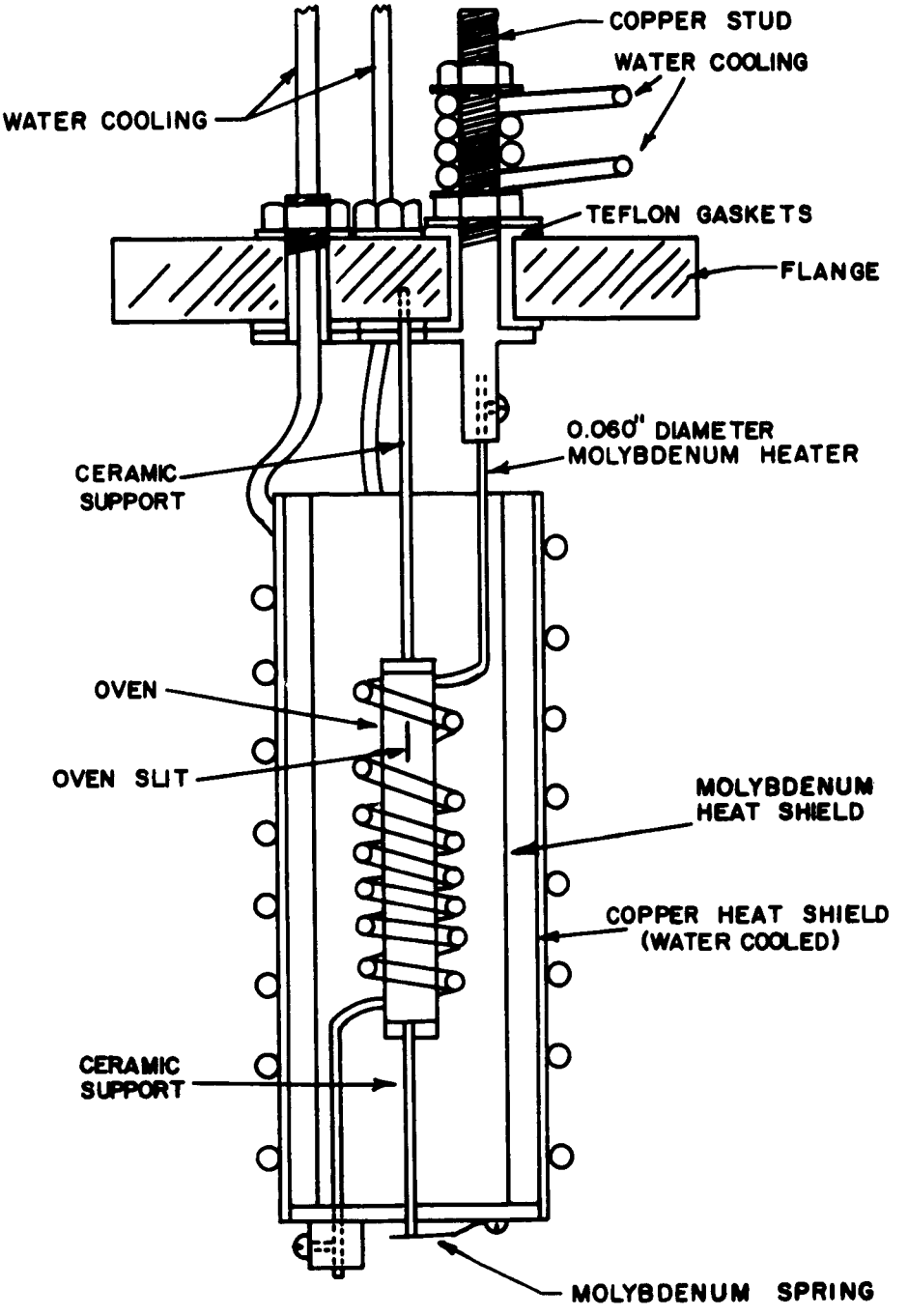

OVEN ASSEMBLY SKETCH

FIGURE 5

The detector chamber is pumped by an ion pump and a liquid nitrogen cold trap. Various detectors may be mounted through a port perpendicular to the beam in this chamber. The ion current output is measured by an electrometer whose output also drives a two-channel recorder. The second channel is used to monitor the oven temperature via a thermocouple. All flanges use copper gaskets for sealing and there are no rubber or similar materials in this part of the system. It was found that the pressure in the detector chamber was approximately 5×10^{-8} mm H with the beam on and about 5×10^{-9} with the gate valve closed.

SECTION 4

MEASUREMENTS OF DETECTOR EFFICIENCY

The detector ionization efficiency may be measured by charging the oven by a known amount of beam material and operating until all the source material has been evaporated. During such a run the oven temperature and the detector ion current were recorded on a two-channel recorder. From these data and knowing the geometry of the machine, it is possible to calculate the ionization efficiency. A run with approximately 5 mg of LiF and an oven slit 10 mm in height, 0.127 mm in width, and 0.8 mm in length lasts about two hours when the source is at 800°C. Figure 6 shows photographs of partial actual recordings of lithium floride on tungsten and thallium on platinum.

The ionization efficiency, η_i, may be derived as follows:

Let I_d = detector current in amperes,

Q_T = total effusion from oven in molecules per second,

W = total oven charge in milligrams,

n = number of molecules per milligram,

e = charge of an electron in coulombs,

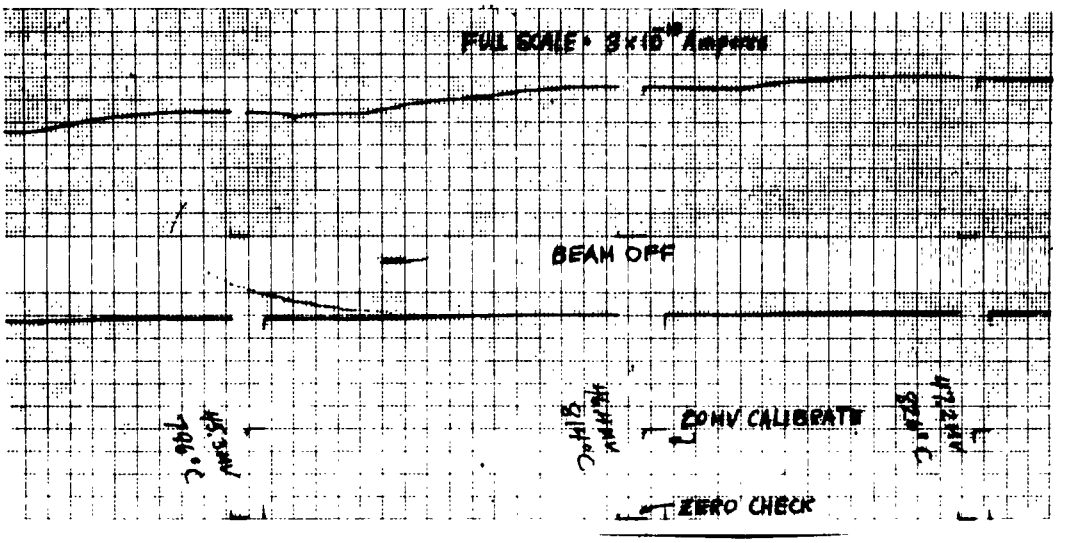

LITHIUM FLUORIDE ON TUNGSTEN

LOWER TRACE IS OVEN TEMPERATURE

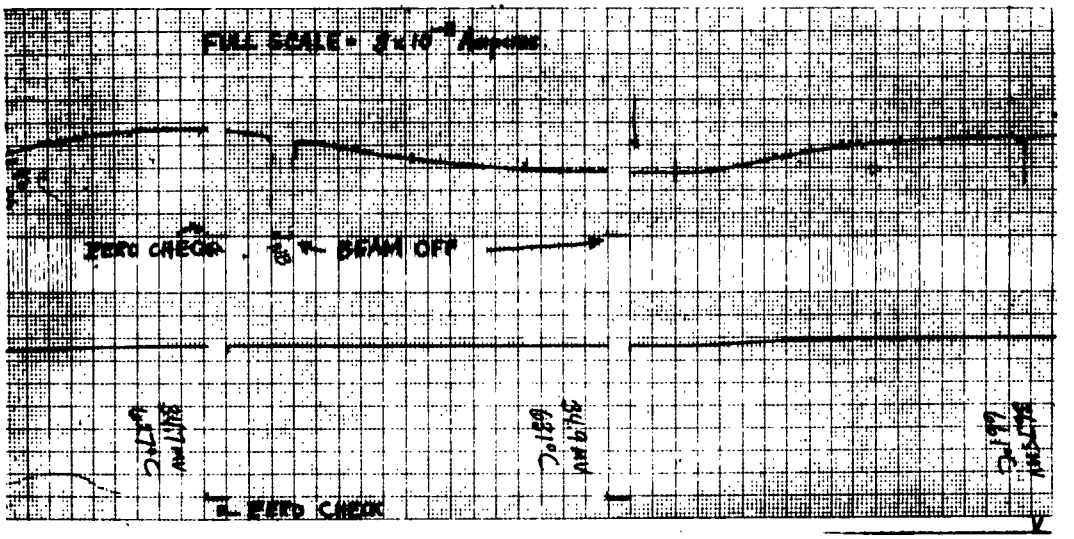

THALLIUM ON PLATINUM

LOWER TRACE IS OVEN TEMPERATURE

Figure 6

f = fraction of molecules reaching the detector,

then

$$I_d = Q_T f \eta_i e, \tag{4-1}$$

and since

$$Q_T = n \frac{dW}{dt}, \tag{4-2}$$

then Eq. (4-1) becomes

$$I_d = n \frac{dW}{dt} f \eta_i e, \tag{4-3}$$

or

$$I_d dt = nfe\eta_i dW. \tag{4-4}$$

Upon integrating both sides of Eq. (4-4), we obtain

$$A = \int_{-\infty}^{\infty} I_d dt = nfe\eta_i W, \tag{4-5}$$

where A = total area under the I_d versus t curve recording, in ampere-seconds. Equation (4-5) yields:

$$\eta_i = \frac{A}{nfeW}, \tag{4-6}$$

where the only unknown quantities are η_i and f.

The fraction, f, of molecules reaching the detector may be determined from the geometry of the machine as follows:

From Ramsay[13] we have

$$Q_T = \frac{1}{K} \frac{1}{4} m \bar{v} A_s \text{ molecules/sec.}, \qquad (4\text{-}7)$$

where

$\frac{1}{K}$ = a tabulated constant depending upon oven slit dimensions,

m = number of molecules per unit volume,

$\bar{v}$ = mean molecular velocity inside source,

A_s = area of source slit.

Assuming that no obstructions intercept the beam on its way to the detector, then the beam intensity, or number of molecules which strike the detector per second, is given by

$$I_B = \frac{1}{4\pi} \frac{A_d}{\ell^2} m \bar{v} A_s \text{ molecules/sec.}, \qquad (4\text{-}8)$$

where

A_d = detector area,

ℓ = distance between source and detector.

Combining Eqs. (4-7) and (4-8) we obtain an expression for f:

$$f = \frac{I_B}{Q_T} = \frac{KA_d}{\pi \ell^2}. \tag{4-9}$$

Substituting Eq. (4-9) into Eq. (4-6) yields

$$\eta_i = \left(\frac{\pi \ell^2}{neKA_d}\right)\frac{A}{W} = \gamma \frac{A}{W}, \tag{4-10}$$

where

$$\gamma = \frac{\pi \ell^2}{neKA_d} \tag{4-11}$$

is a constant depending upon the beam material used and the geometry of the machine. A is the area under the ion current versus time recording and may be obtained by a graphical integration; W is the oven charge in milligrams. Results of the efficiency measurements are given in Section 7.

SECTION 5

MEASUREMENTS OF VAPOR PRESSURE

Equation (4-8) of the preceding Section may also be expressed in another form (Ramsay[13]):

$$I_B = 1.12 \times 10^{22} \frac{pA_sA_d}{\ell^2\sqrt{MT_{ov}}} \text{ molecules/sec.,} \qquad (5\text{-}1)$$

where

p = the source pressure in mm Hg.

M = the molecular weight,

T_{ov} = the oven temperature in ^oK,

A_s = source slit area in cm^2,

A_d = detector area in cm^2,

ℓ = distance between source and detector in cm.

The detector ion-current is given by

$$I_d = I_B \eta_i e, \qquad (5\text{-}2)$$

if one assumes singly ionized molecules.

Combining Eqs. (5-1) and (5-2), and solving for p, we obtain

$$p = \left[2.26 \times 10^5 \frac{\sqrt{M}}{\eta_i}\right]\sqrt{T_{ov}}\, I_d \text{ mm Hg.} \qquad (5\text{-}3)$$

As seen one may therefore obtain the oven pressure or vapor pressure versus temperature if the ionization efficiency is known. In fact, one may substitute for η_i in Eq. (5-3) from Eq. (4-10) and get

$$p = \left[2.26 \times 10^5 \frac{\sqrt{M}}{\gamma}\frac{W}{A}\right]\sqrt{T_{ov}}\, I_d. \qquad (5\text{-}4)$$

By recording I_d versus T_{ov}, p versus T_{ov} may be obtained by E. (5-4). If log p is plotted versus $(T_{ov})^{-1}$ and a straight line results, then this line may be fitted to the so-called "Antoine Equation" for vapor pressure versus temperature:

$$\log_{10} p = a - \frac{b}{T}, \qquad (5\text{-}5)$$

where a and b are constants which may be determined from the log p versus $\frac{1}{T}$ graph.

Results are given in Section 7.

SECTION 6

MEASUREMENT OF WORK FUNCTIONS

Under certain conditions it may be permissible to assume that surface ionization principally takes place by the Saha-Langmuir mechanism. In other words, other processes contribute a negligible amount to the ion current observed and its temperature dependence. Assuming that it is permissible to define an average work function, ϕ, of the hot wire, we then have:

$$\frac{n_+}{n_a} = \frac{1 - r_+}{1 - r_a} \frac{w_+}{w_a} \exp\left[\frac{e(\phi - I)}{kT}\right]. \qquad (6\text{-}1)$$

If $I > \phi$, $n_+ << n_a$, and n_a is approximately constant (see Fig. 1), then it is valid to write

$$\ell n\ n_+ = \ell n\ n_a \frac{w_+}{w_a} \frac{1 - r_+}{1 - r_a} + \frac{e}{kT} (\phi - I). \qquad (6\text{-}2)$$

Assuming, further, no temperature-dependent reflections, Eq. (6-2) becomes

$$\ell n\ n_+ = \text{constant} + \frac{e}{kT} (\phi - I). \qquad (6\text{-}3)$$

Since the ion current is proportional to n_+, upon plotting $\ell n\ n_+$ versus $\frac{e}{kT}$ one should obtain a straight line with a slope equal to $\phi - I$. If $I = \phi$, the exponential term becomes a constant and the ion current is independent of T; hence, the slope of the $\ell n\ n_+$ versus $\frac{1}{T}$ curve is zero. If $I < \phi$, the ionization is practically 100% and the slope again is zero.

Conditions under which one may use the Saha-Langmuir law of surface ionization are probably obtained when dealing with an atomic (as opposed to a molecular) beam under ultra-high vacuum conditions such that the filament has a good chance to clean up before the experiment is conducted.

SECTION 7

EXPERIMENTAL RESULTS

Ionization of LiF and Li

Several runs of LiF with a tungsten detector were made over a period of 2 months in order to become familiar with the operation of the machine. During these runs it was found that the ionization efficiency varied considerably from run to run. This was found to be partly due to incorrect alignment of the oven with the beam-defining slit and the detector. By checking the alignment with the beam itself several times during a run, it was found that this parameter could be controlled very closely. Still it was found that the efficiency varied widely between runs. By operating the filament continuously at 1350^{o}K in 5 x 10^{-9} mm Hg for about a week, three runs in succession gave ionization efficiency results differing by no more than 10%, (i.e., 12.5%, 13.5%, and 13.75%). These runs were spaced one day apart and the filament was left on at all times. Turning off the filament current for short periods of time between runs proved to be the main cause of getting different ionization efficiencies for different experiments.

Figure 7 shows the measured vapor pressure of LiF versus 1000/T, T in ^{o}K. The reason for the departure of the curve from a straight line at higher temperatures, (i.e., high pressures), is that the mean free path of the molecules inside the oven becomes comparable to the slit width. When this happens, a partial hydrodynamic flow results with the creation of a turbulent gas jet instead of free molecular flow or effusion, and an increasingly (with temperature) large fraction of the effusing molecules collide with each other either in the source slit or immediately after they emerge. In this way, a cloud of molecules is formed in front of the slit whose boundary serves as the effective source. As the source pressure is increased, the cloud increases more in size than in intensity; hence, the beam is broadened and the intensity is not increased in the same ratio as the pressure (see also Reference 13). The knee in the curve may be used to estimate the molecular scattering cross-section.

From the kinetic theory of gases it is found that

$$\lambda_m = \frac{1}{4\sqrt{2}\ \sigma N} \text{ meters}, \qquad (7\text{-}1)$$

where

λ_m = molecular mean free path in meters,

σ = molecular scattering cross-section = πr^2 in meters^2,

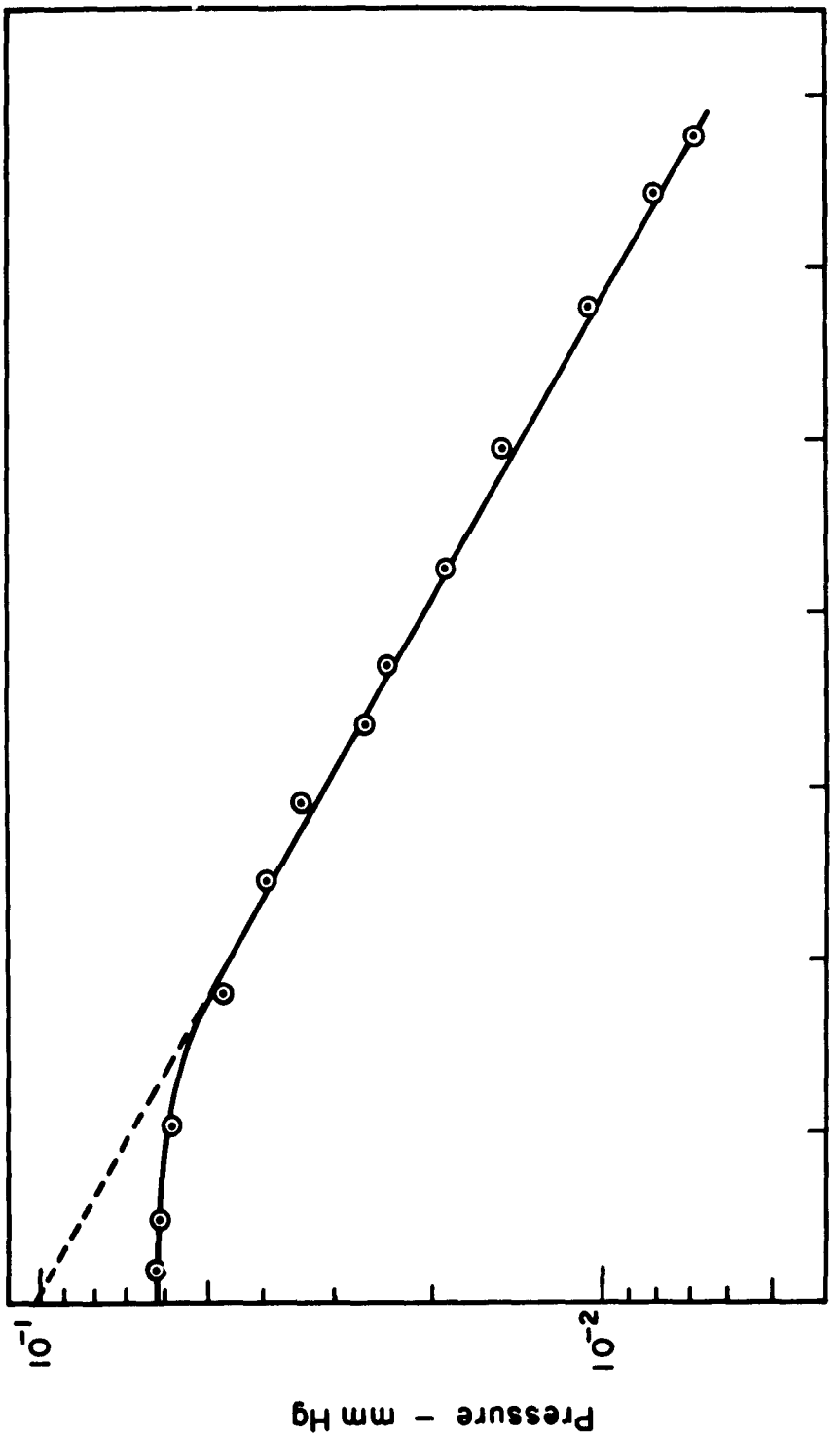

VAPOR PRESSURE OF LITHIUM FLUORIDE

Figure 7

r = molecular radius in meters,

N = number of molecules per unit volume.

The concentration, N, is given by

$$N = 9.68 \times 10^{24} \frac{P}{T} \text{ molecules/m}^3, \qquad (7\text{-}2)$$

where

p = pressure in mm Hg,

T = temperature in ^{o}K.

Combining Eqs. (7-1) and (7-2) and solving for σ, we obtain

$$\sigma = 1.83 \times 10^{-26} \frac{T}{p\lambda_m} \text{ meters}^2. \qquad (7\text{-}3)$$

The knee in the curve of log p versus $\frac{1}{T}$ occurs when

$$\lambda_m \simeq w,$$

where

w = width of the oven slit.

Hence, from the vapor pressure data it is possible to estimate λ_m at a given temperature and pressure, and therefore calculate σ by Eq. (7-3). The results are given in Table I. For comparison purposes values of the scattering cross-sections as computed by using $\sigma = \pi r^2$ with r obtained from published data[21] are also tabulated.

TABLE I

MATERIAL	EXPERIMENTAL σ IN cm^2	CALCULATED FROM πr^2 IN cm^2	RADIUS USED IN CALCULATIONS. r IN ANGSTROMS
Li	5.81×10^{-16}	7.6×10^{-16}	1.56
Tℓ	*19×10^{-16}	12.6×10^{-16}	1.99
LiF	262×10^{-16}	---	---

The ionization efficiency for the run used to obtain the data for Fig. 7 was found to be 13.75% with a 1-mil diameter tungsten wire. Using this graph to obtain numerical values for the constants a and b in Eq. (5-5) results in

$$\log_{10} p = 7.06 - \frac{8950}{T}, \qquad (7\text{-}4)$$

where

p = vapor pressure in mm Hg,

T = temperature in ^{o}K.

A second run on LiF was used to obtain the variation of ion-detector current versus electric-field intensity at the detector wire. According to Eq. (2-10) the ion current should vary as exp $\sqrt{E}$. In Fig. 8 the ion current

*Estimated to be a maximum value only since the knee in the log p vs 1/T curve for thallium was obtained by extrapolation.

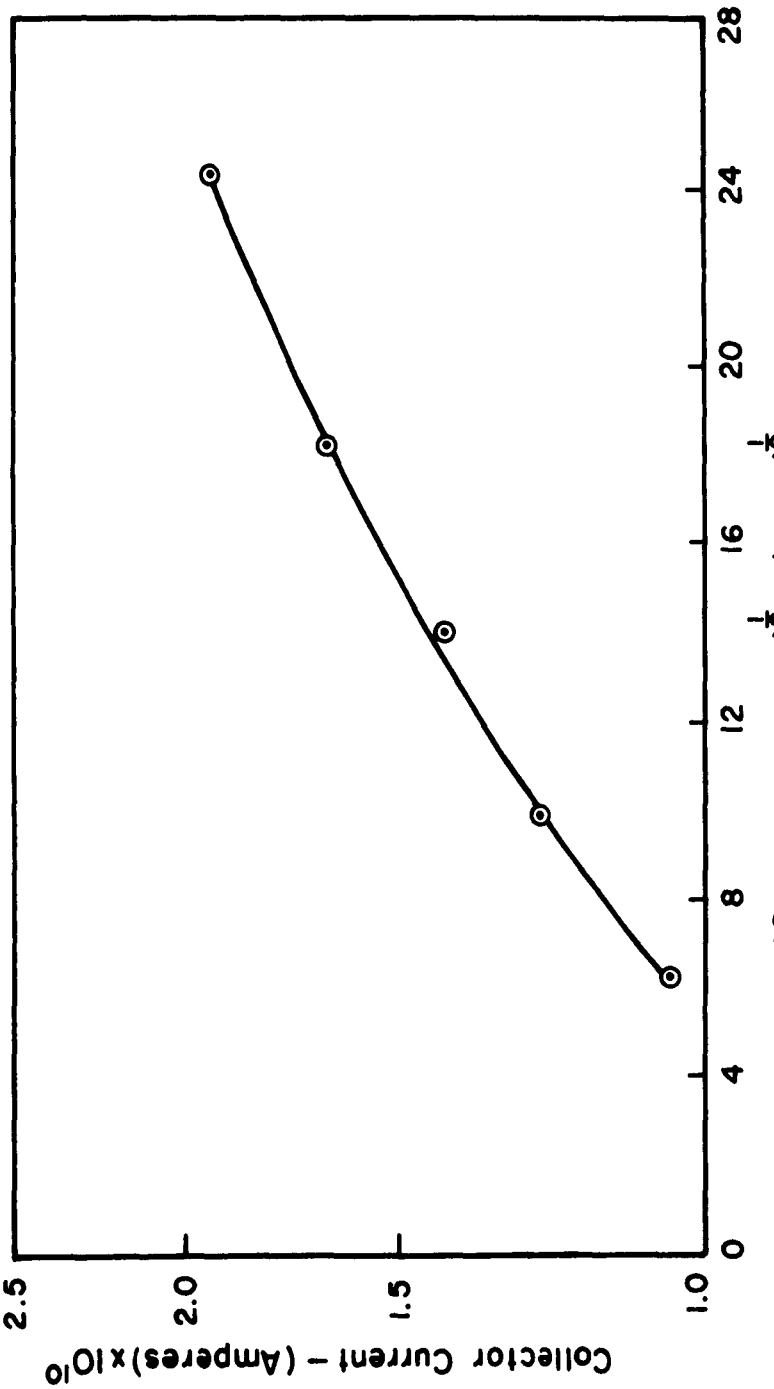

DETECTOR ION CURRENT VS. (COLLECTOR VOLTAGE)$^{\frac{1}{2}}$

Figure 8

is plotted on a logarithmic scale versus the square-root of the collector voltage. As may be seen, a good approximation to a straight line results, which seems to indicate good correlation between the experimental results and those predicted by Eq. (2-10). On the other hand, we found that increasing the filament temperature resulted in an increase in the ion current (at constant beam flux) but that this increase was of a transient nature, decaying exponentially back to approximately its original value before the increase took place. Similarly, a decrease in filament current resulted in momentary decrease in ion current which then would increase exponentially back to its previous value. In other words, under thermal equilibrium the ion current was, for all practical purposes, constant over a wide range of filament temperatures.

For comparison purposes a beam of Li on a 1-mil tungsten wire was run. Figure 9 shows the vapor pressure as measured for Li. The ionization efficiency was found to be only 1.15% for this run with the filament at 1350^{o}K.

The next set of runs consisted of LiF on the following metals: a 3-mil diameter wire drawn from a single tungsten crystal, a 3-mil diameter wire of rhenium, and a 1-mil diameter wire of platinum. Two runs were made with the rhenium wire, one immediately after high vacuum condition was obtained, the other after about a week of degassing the rhenium filament at approximately 1400^{o}K

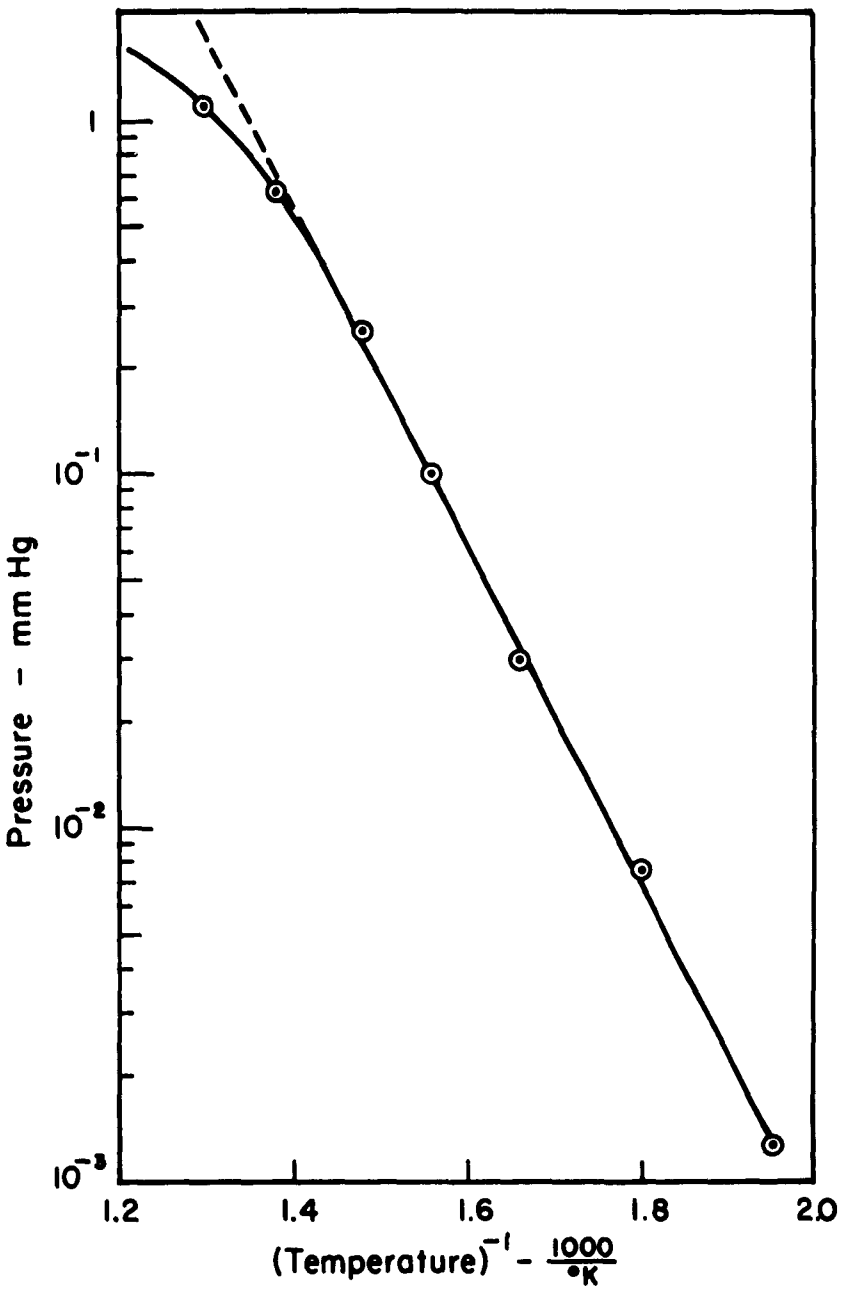

VAPOR PRESSURE OF LITHIUM

Figure 9

in 5 x 10^{-9} mm Hg pressure.

The results are plotted in Fig. 10. The ordinate is the detector-ion current on a logarithmic scale, the abscissa 1000/T, where T is the oven temperature in ^{o}K.

As may be seen from this figure, the ionization efficiency is highest for ordinary tungsten (13.8%). Tungsten wire drawn from a single crystal shows an efficiency almost as high, namely 11.3%. The efficiency on rhenium on the first run (i.e., before outgassing took place), is only about 0.5%. After clean-up of the rhenium filament the efficiency increased by almost an order of magnitude; i.e., to 3.75%. The ionization efficiency for LiF on well aged platinum was found to be approximately 2-2.5%. These efficiencies were calculated at relatively low beam intensities. At higher beam intensities, the efficiencies on rhenium and platinum are almost as high as that of tungsten, as may be seen from the curves in Fig. 10. In other words, the slope of the curves for rhenium and platinum are higher (negative slopes) than those for tungsten.

As mentioned above, the ion current for LiF on tungsten was found to be practically independent on filament temperature. This was not found to be the case for LiF on well degassed and aged platinum.

Figure 11 shows the variation of the detector ion-current for LiF on platinum. As may be seen, there is a

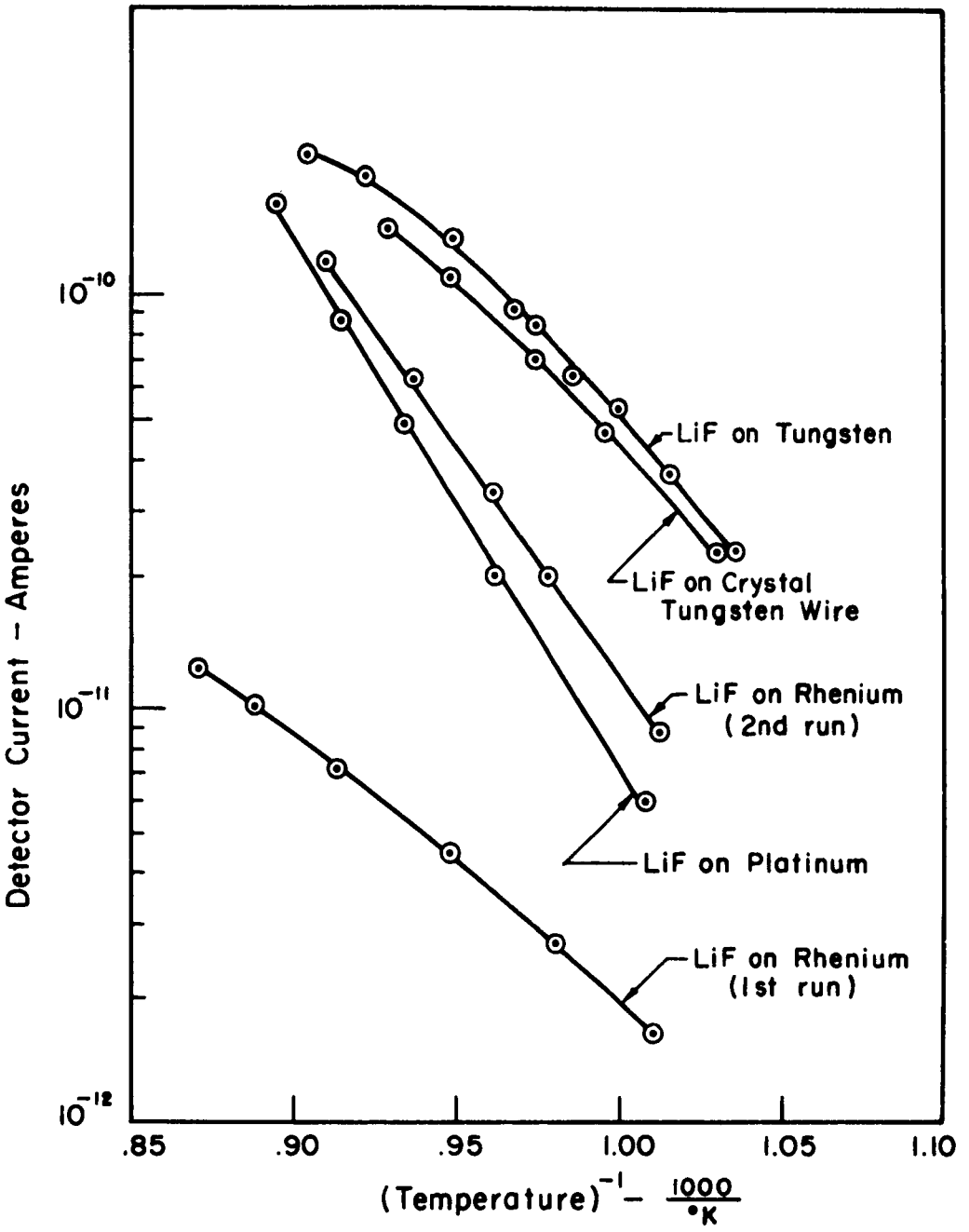

DETECTOR ION CURRENT VS. (OVEN TEMPERATURE)$^{-1}$

Figure 10

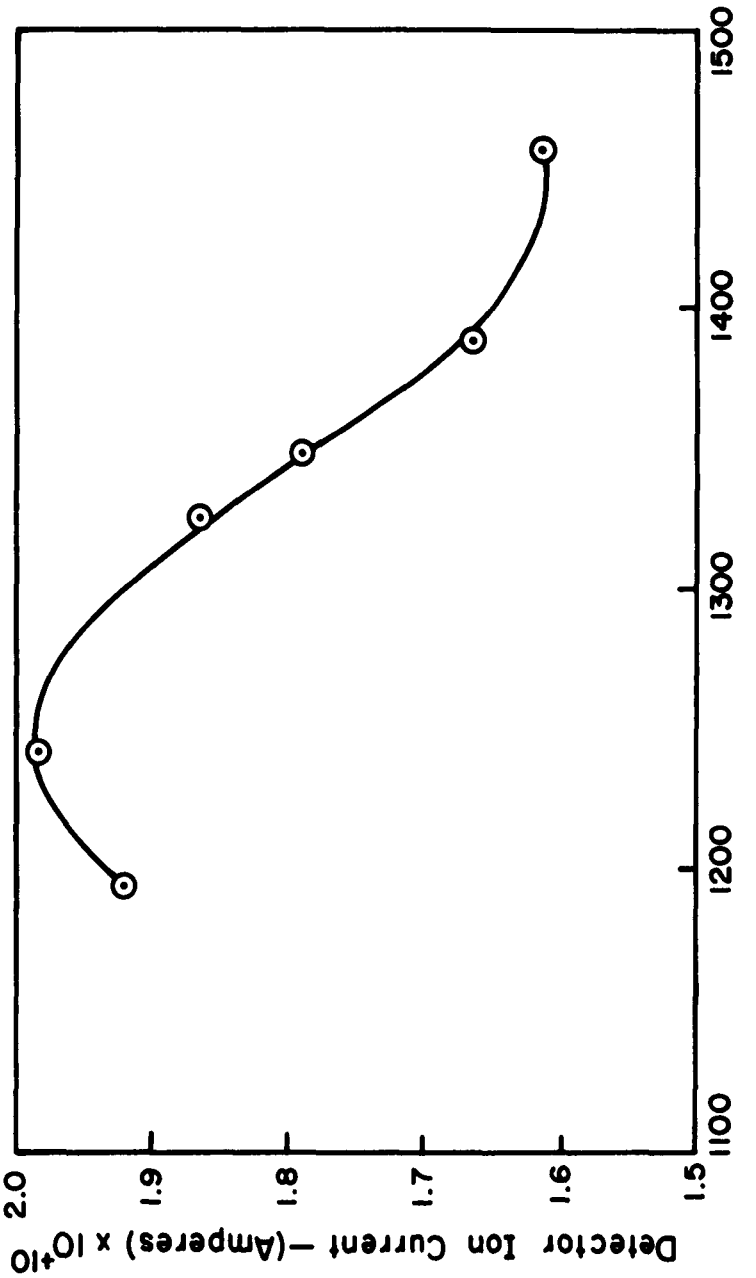

DETECTOR ION CURRENT VS. FILAMENT TEMPERATURE

LITHIUM FLUORIDE ON PLATINUM

Figure 11

definite maximum in the curve, occurring at about 1250°K. To explain this maximum one may reasonably assume that the ionization probability is proportional to the filament temperature and to the length of time an atom spends on the surface before being evaporated either as an ion or as a neutral atom. The condition of high temperature and long adsorption time is incompatible, since the sticking time decreases with an increase in temperature. We would, therefore, expect to see a maximum in the ion current when the filament temperature is varied. This type of behavior apparently can only be detected for ultra-clean filaments and for the case of a molecule, such as LiF, since the presence of fluorine allows for the possibility of chemical reactions to take place on the surface and these chemical reactions are, in all probability, time dependent. A more careful run of LiF on tungsten showed a small peak also but not as pronounced as that found on platinum. For comparison purposes, a beam of Li was run on platinum. Surprisingly enough, the behavior of the detector ion current versus filament showed a definite maximum again, but at a lower temperature (see Fig. 12). The maximum ionization efficiency occurred at about 1150°K and was found to be approximately 1.27%.

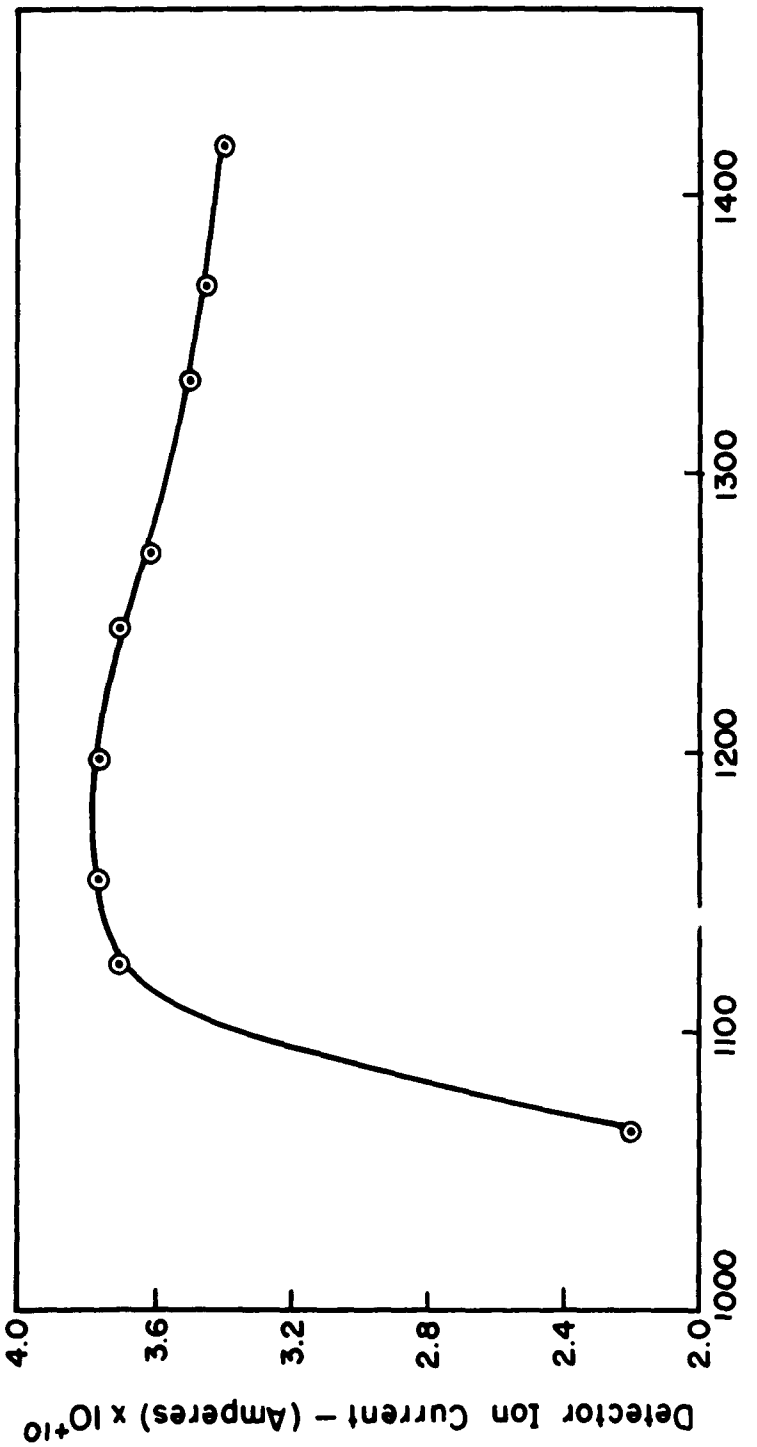

DETECTOR ION CURRENT VS. FILAMENT TEMPERATURE

LITHIUM ON PLATINUM

Figure 12

SECTION 8

IONIZATION OF THALLIUM

Due to the increased interest in thallium as a possible atomic-beam frequency standard the ionization efficiency of thallium on tungsten, rhenium, and platinum was measured. The vapor pressure of thallium was also obtained.

For a well aged and cleaned tungsten filament the ionization efficiency was found to be so low that no reliable measurement could be made. The average signal amplitude was approximately equal to the average noise amplitude. On the other hand, rhenium and platinum were found to make good detectors for thallium.

Figure 13 shows the detector ion-current on a logarithmic scale versus 1000/T, T being the oven temperature in ^{o}K. The measured efficiency of rhenium is 0.0475% at a filament temperature of 1700^{o}K, and that for platinum 0.245% at a filament temperature of 1365^{o}K. Previous to the runs the filaments were out-gassed at about 1400^{o}K for the platinum and at 1800^{o}K for the rhenium for about four days in a vacuum of 5×10^{-9} mm Hg. A second run of thallium on platinum was made after letting the filament outgas an

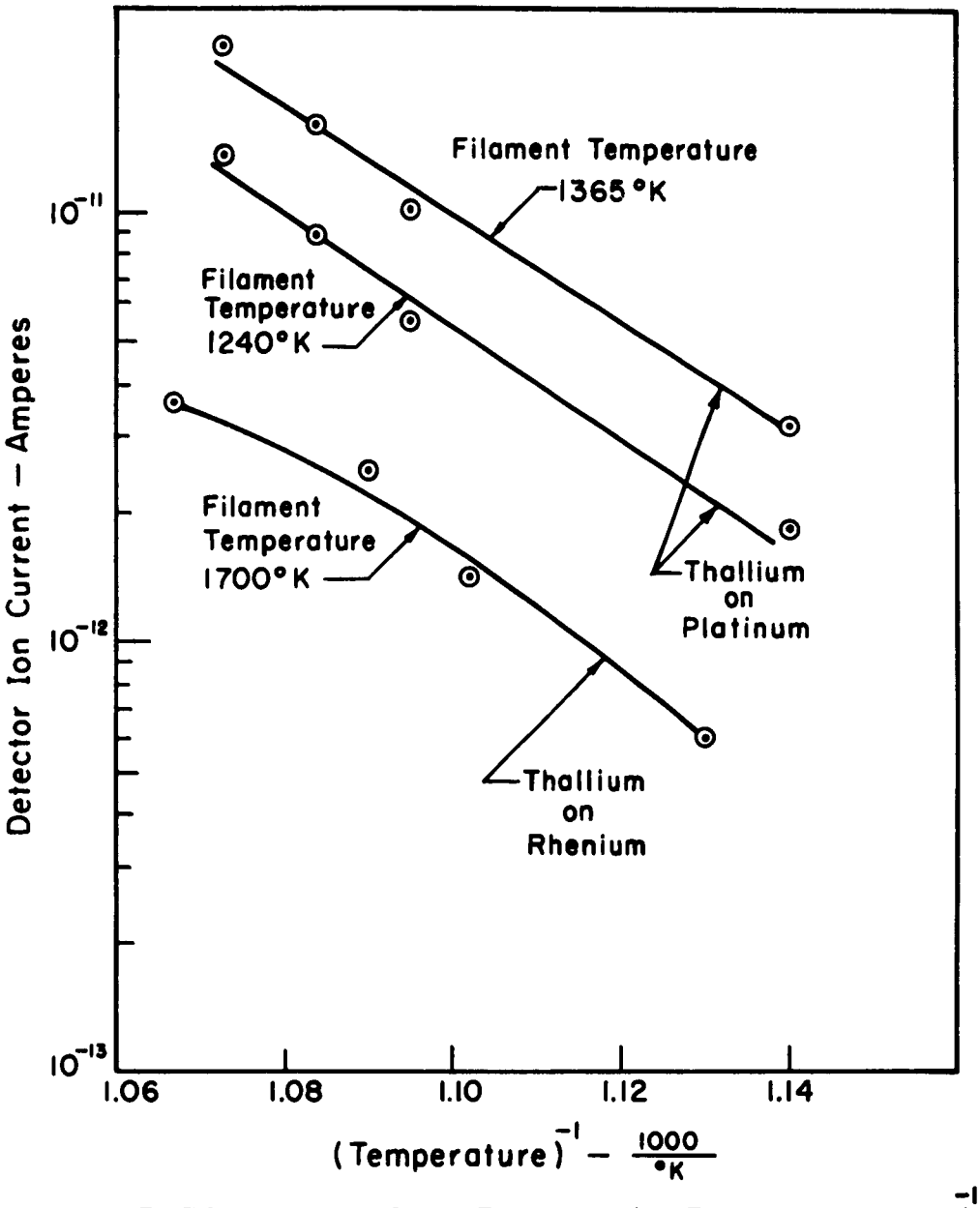

DETECTOR ION CURRENT VS. (OVEN TEMPERATURE)$^{-1}$

THALLIUM ON RHENIUM AND PLATINUM

Figure 13

an additional four days. The result is shown in Fig. 14. The efficiency was found to be much higher than before; i.e., 0.84% at a filament temperature of 1365^{o}K, and with a signal-to-noise ratio of about 40:1.

Figure 15 shows the variation of the detector-ion current versus 1000/T, T being the filament temperature in ^{o}K. Since the variation is a straight line on a log I versus $\frac{1}{T}$ plot, it is reasonable to assume that the ionization takes place by the Saha-Langmuir mechanism. If that is indeed the case, then one may obtain the difference between the work function of platinum and the ionization potential of thallium. Assuming an ionization potential of 6.07 volts for thallium the slope in Fig. 15 yields a work function of 5.34 volts for platinum which compares reasonably well with other published data[21] (i.e., ranging from 5.08 to 6.27 volts).

Figure 16 shows the vapor pressure of thallium over the range 555^{o}C to 729^{o}C.

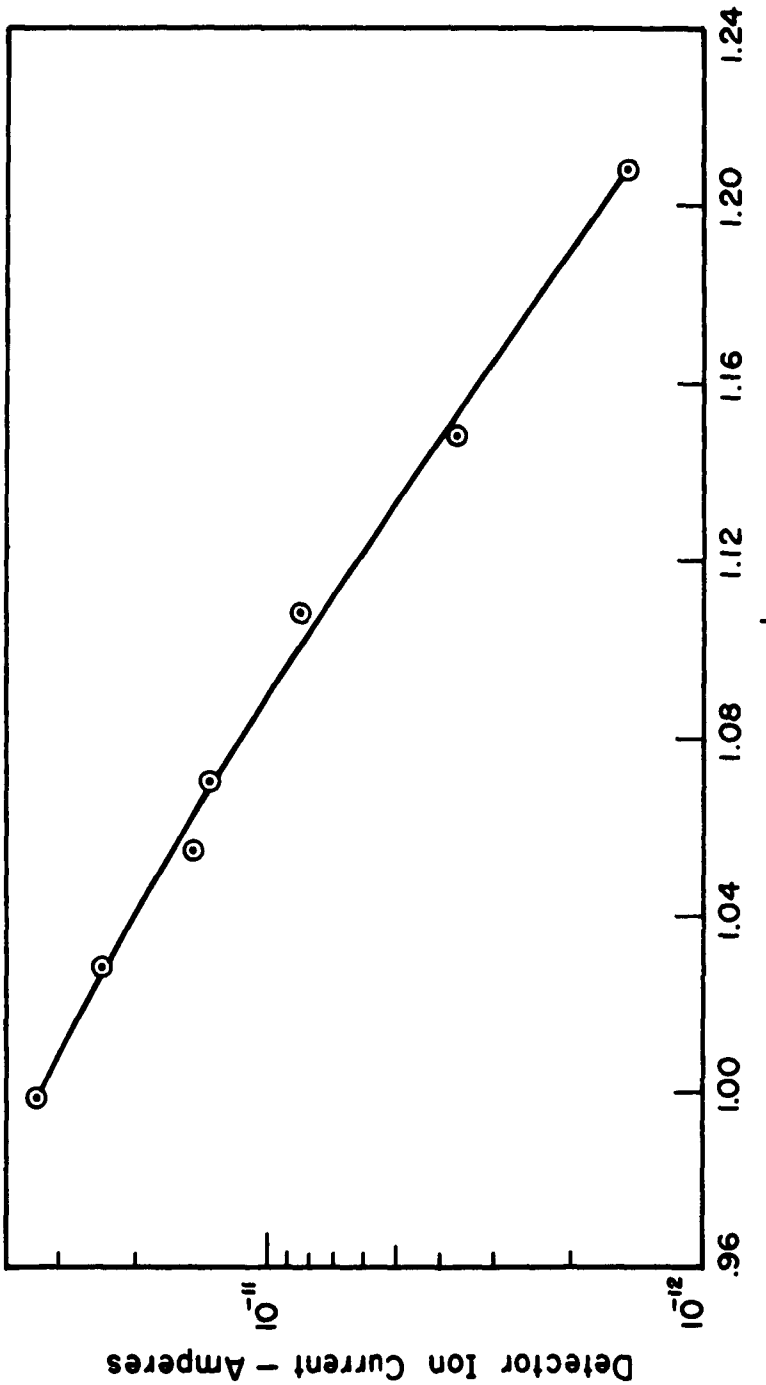

DETECTOR ION CURRENT VS. (OVEN TEMPERATURE)$^{-1}$

THALLIUM ON PLATINUM

Figure 14

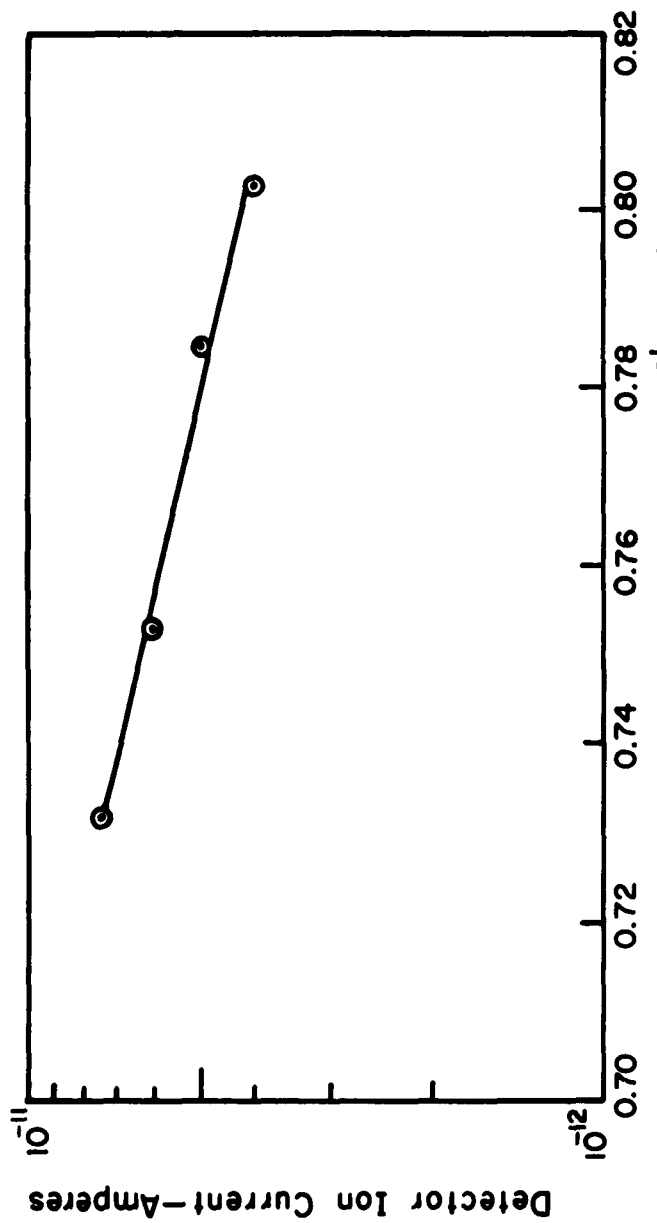

DETECTOR ION CURRENT VS. (FILAMENT TEMPERATURE)$^{-1}$

THALLIUM ON PLATINUM

Figure 15

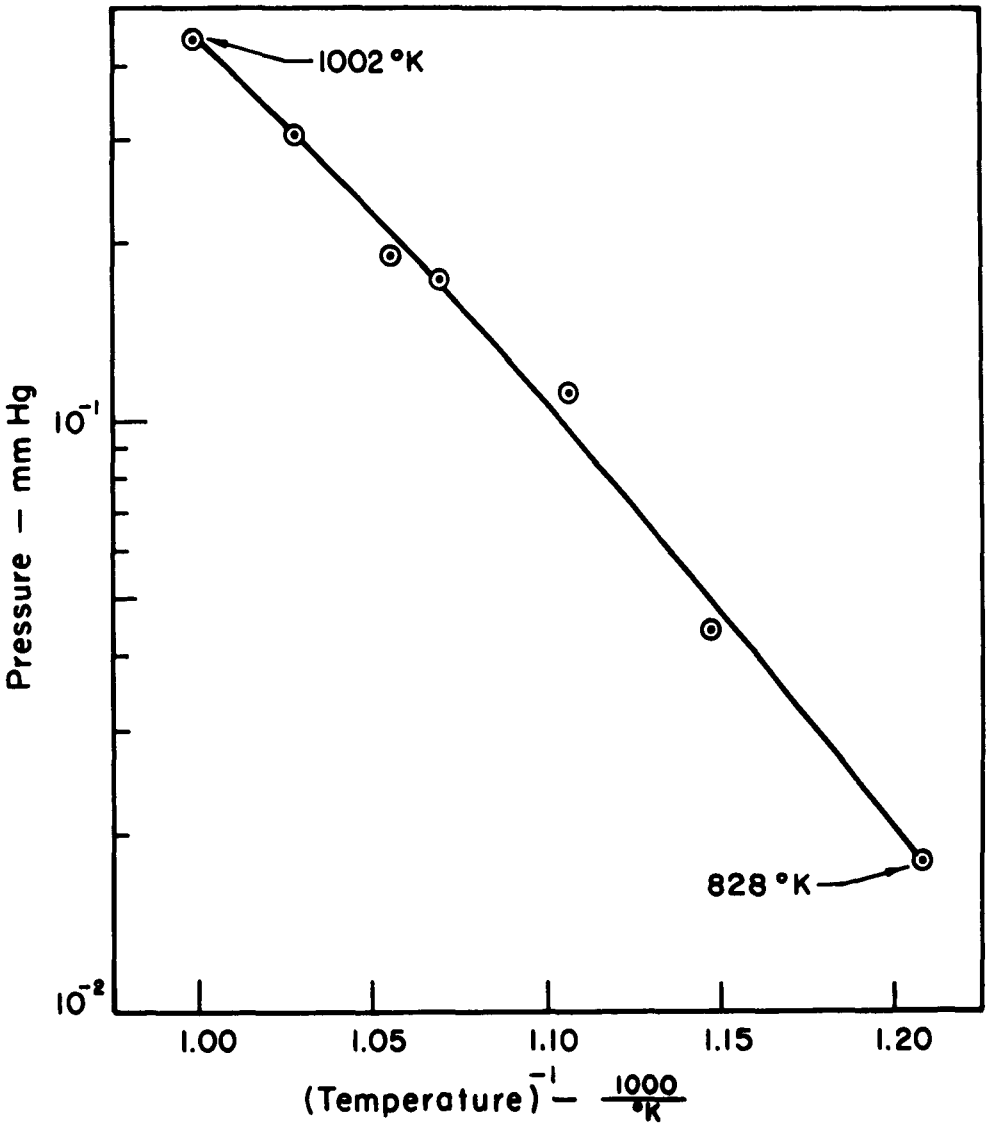

VAPOR PRESSURE OF THALLIUM

Figure 16

SECTION 9

ADDITIONAL THEORETICAL CONSIDERATIONS

Possibility of Ionization by Tunneling

Figure 17 shows the potential diagram for an electron of an atom near a metal surface. As may be seen, the potential barrier at the surface is reduced in both thickness and height by the presence of the atom and the applied field. If the barrier is thin enough, there exists a finite probability that an electron may tunnel through the barrier from the atom into the metal and produce a positive ion which may be desorbed.

Tunneling is a purely quantum-mechanical phenomenon with no classical analog.[14] It can best be reconciled with macroscopic intuition by the Heisenberg uncertainty principle:

$$\Delta p \Delta x \geq \frac{\hbar}{2}, \tag{9-1}$$

where Δp is the uncertainty of the knowledge in the momentum of an electron, Δx the corresponding uncertainty in position, and $\hbar = \frac{h}{2\pi}$, h being Planck's constant.

If we consider electrons with an uncertainty in momentum corresponding to the ionization potential I (i.e.,

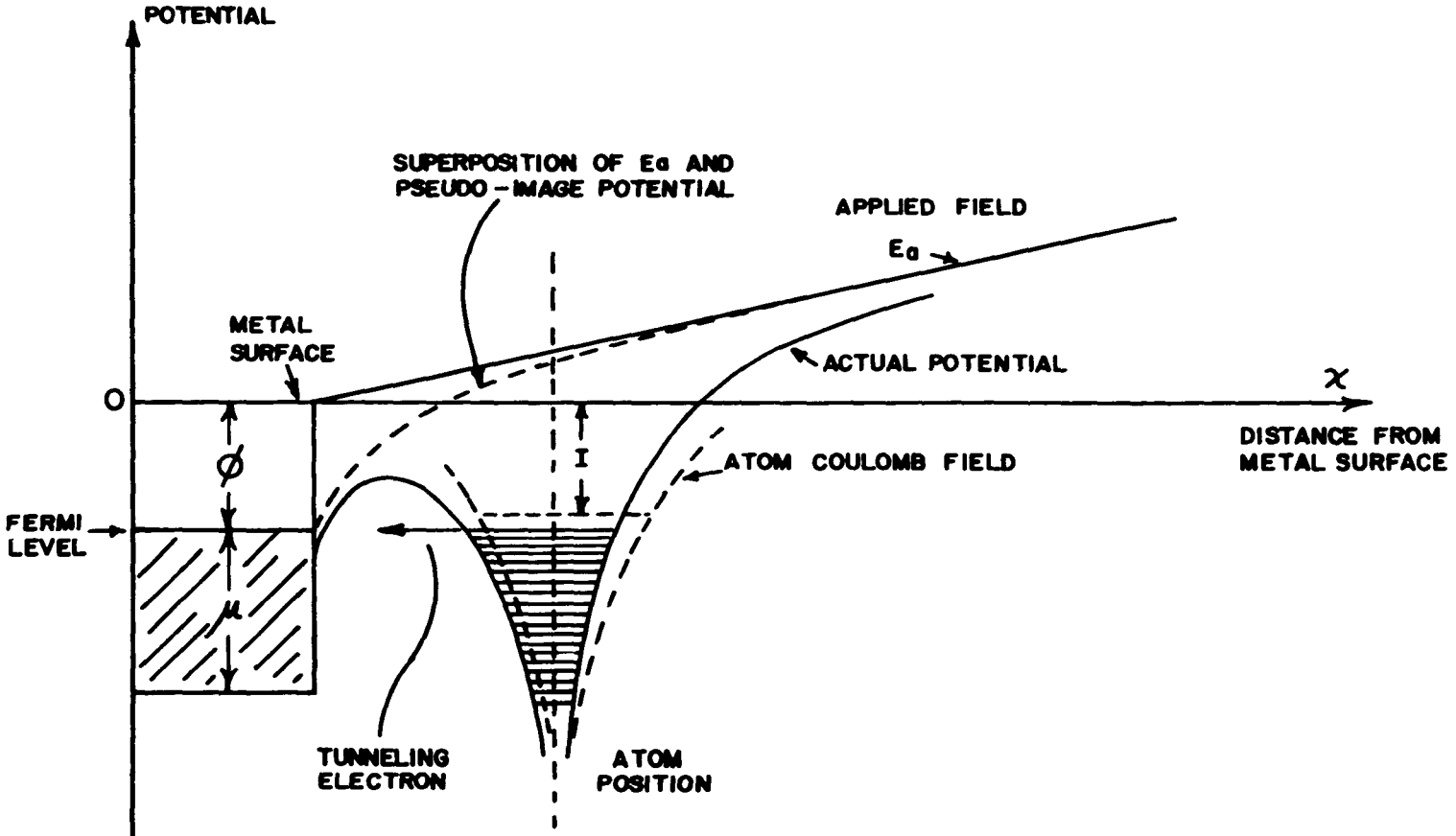

POTENTIAL DIAGRAM OF AN ATOM NEAR A METAL SURFACE

Figure 17

$(2mI)^{1/2}$), and if we find that the uncertainty in position

$$\Delta x = \frac{h}{2} \frac{1}{(2mI)^{1/2}} \qquad (9\text{-}2)$$

is of the order of the barrier width, then there will be a good chance of finding the electron on either side of it. Penetration coefficients for a one dimensional barrier can be found by the Wentzel-Kramers-Brillouin, (WKB[14]) method, and the result is

$$A = f(E,V) \exp \left[- \frac{2\sqrt{2m}}{h} \int_o^{\ell} (V - E)^{1/2} dx \right], \qquad (9\text{-}3)$$

where

A = probability that an electron traveling to the left will not be turned back,

V and E are the electron's potential and kinetic energies respectively,

f(E,V) is an insensitive function of V and E that often can be approximated by unity, and

ℓ is the tunneling length.

The exponent in the right-hand member of Equ. (9-3) represents, apart from the factor $\frac{2\sqrt{2m}}{h}$, the area under the curve with ordinate $(V - E)^{1/2}$ from $x = 0$ to $x = \ell$.

Before proceeding further, let us examine how close to the metal surface an atom will approach. Figure 17 shows the closest approach of an atom to a metal surface

at which tunneling can occur in a given field. The reason for this is the absence of empty states below the Fermi level. The potential barrier is the total field due to the applied electric field, the image potential of the electron and the positive nucleus, and the coulomb field of the atom. The image potential is very small when the distance of the electron and the nucleus are approximately the same. These distances are very small and the image potential energy may be approximated by

$$V_{image} \cong \frac{e^2}{16\pi\epsilon_o x} \cong \frac{3.6}{x} \text{ volts } (x \text{ in } \mathring{A}). \qquad (9\text{-}4)$$

If we let the closest approach be x_c, then since the applied field must raise the tunneling electron to μ (μ = Fermi level), we obtain

$$x_c = \text{thickness of barrier} \cong \frac{I - \phi}{E_a}, \qquad (9\text{-}5)$$

where E_a = applied field in volts/m.

A simple calculation shows that the maximum applied field intensity for the detector used in our experiments is only of the order of 0.001 V/$\mathring{A}$, therefore

$$x_c \cong 1000(I - \phi)\mathring{A}, \qquad (9\text{-}6)$$

which means the barrier is thick, usually too thick for

tunneling to take place, unless $I - \phi$ is very small.

The above considerations probably apply only to atoms and not to molecules such as LiF (or other alkali halides). For a diatomic molecule the picture is more complex.

Possibility of an increase in work function due to a dipole surface layer.

A possible explanation for the observed increased efficiency of LiF as compared to Li may be due to the fact that the work function, ϕ, of a metal is increased if an electro-negative ion, such as fluorine, is adsorbed on the surface.

The potential difference encountered by electrons in going through a dipole layer as shown in Fig. 18 may be found considering a parallel plate capacitor with a surface charge density ρ_s; then

$$D_n = \rho_s, \text{ or } E_n = \frac{\rho_s}{\epsilon_o}, \tag{9-7}$$

where:

D_n = electric flux density normal to the plates,

E_n = electric field intensity normal to the plates.

The potential difference between the plates is

$$\Delta V = \int \overline{E} \cdot d\overline{l} = \frac{\rho_s}{\epsilon_o} d, \tag{9-8}$$

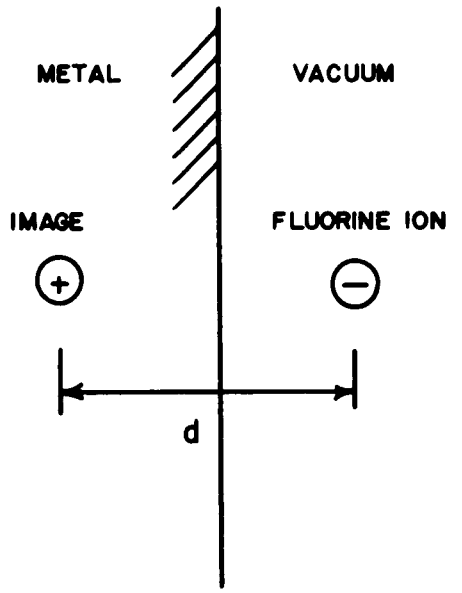

NEGATIVE FLUORINE ION ADSORBED ON A METAL SURFACE

FIGURE 18

where:

d = spacing between the plates.

Now, assuming that

$$\rho_s = Ne, \tag{9-9}$$

where

N = number of negative ions adsorbed per unit area,

we obtain

$$\Delta V = \frac{Ned}{\epsilon_o} = \frac{NP}{\epsilon_o}, \tag{9-10}$$

where

P = dipole moment.

The effective work function is, therefore,

$$\phi' = \phi + \frac{NP}{\epsilon_o} . \tag{9-11}$$

Let us estimate the <u>maximum</u> value of $\frac{NP}{\epsilon_o}$. Assuming that d is equal to twice the radius of the F^- ion, we obtain ($d = 2 \times 1.36$ Å)

$$P_{max} = ed = 4.35 \times 10^{-29} \text{ coulomb-meter.} \tag{9-12}$$

Let us also assume a surface density such that the distance

between neighboring F^- ions is also twice their radii; then

$$N_{max} = \left[\frac{10^{10}}{2(1.36)}\right]^2 = 1.35 \times 10^{19} \text{ ions/m}^2. \tag{9-13}$$

This yields

$$\left[\frac{PN}{\epsilon_o}\right]_{max} = 66 \text{ volts}, \tag{9-14}$$

which certainly seems to indicate the possibility for increasing the work function by a few tenths of a volt, which may account for the increase in ionization efficiency for LiF as opposed to Li if we can assume that the ionization takes place by the Saha-Langmuir mechanism.

In the case of the alkali-halides there are two overall possibilities for ionization, either direct ionization of the molecule MX to MX^+, or preliminary dissociation followed by ionization of the atom. Direct ionization of the molecule is not likely due to the high ionization potentials of the alkali-halides and will not be considered. The second process, dissociation followed by ionization of the atom, is the more likely method; and if the steps of the process are in chemical and thermal equilibrium, then the ratio of ions to neutral atoms should be given by the Saha-Langmuir equation using the ionization potential of the alkali atom and the work function proper for the site of desorption. LiF should conform to this at very high

filament temperatures and should be ionized by approximately the same efficiency as Li. At lower temperatures, where some coverage by fluorine is very likely, the efficiency should be much higher for LiF than Li as observed. Evidence for dissociation preceding ionization for alkali-halides on tungsten is given by Ionov[15] who found that the electron affinity of Cl measured by negative ion formation by tungsten from alkali-chlorides was independent of the cation (Na, Rb, K, or Cs). Datz and Taylor[16] have investigated ionization of the potassium-halides on tungsten and platinum surfaces and find that the potassium-halides on tungsten seem to conform to the Saha-Langmuir equation; i.e., that the ionization efficiencies of the potassium-halides (KF, KI, KBr, and KCℓ) are at high temperatures essentially identical with the values for elemental potassium. At lower temperatures they find higher efficiencies which they ascribe to a partial coverage of the tungsten surface by halogen. They also find that the results on platinum differ markedly from those expected from the Saha-Langmuir equation and those on tungsten. To explain the ionization efficiencies for KI, KBr and KCℓ on platinum they assume large reflections strongly dependent upon chemical factors to be operative. Finally, they find a marked divergence of KF from the other three halides on platinum which they assume to be due to some special platinum-flourine interaction.

These data seem to be somewhat similar to what we have observed in the case of LiF on tungsten and platinum. The results on platinum is markedly different than those on tungsten with respect to the behavior of the ionization efficiency versus filament temperature.

SECTION 10

CONCLUSIONS

The principal conclusion of this work of engineering importance is that lithium fluoride and thallium can be detected with high signal-to-noise ratios on well aged platinum wires. In order to obtain these large signal-to-noise ratios the filament has to be allowed sufficient time at high temperatures in high vacuum (of the order of 10^{-8} mm Hg or better). The signal-to-noise ratio as well as the ionization efficiency both increase with the degree of clean-up of the filaments. Furthermore, the noise due to the background gases in the vacuum system decreases with a reduction of the pressure; this again calls for the use of ultra high vacuum techniques.

We have demonstrated that the experimental methods used are practical for the measurements of ionization efficiencies, vapor pressure, and, in some cases, work functions of the filaments used. With the application of an electric field intensity of about 5000 volts/mm at the detector surface it is possible to approximately double the ionization efficiency. Unfortunately, this also increases the noise level, and the net gain in signal-to-noise ratio is not significant.

The postulated explanation in terms of an adsorbed dipole layer apparently accounts for most of the observed deviations from the Saha-Langmuir ionization equation. The possible special platinum-fluorine interaction should be studied in greater detail. This may possibly be done by a mass-spectrometer analyzing the ion current, by another mass-spectrometer analyzing the constituents of the vacuum system, and possibly by the use of a field-emission microscope to study the platinum surface in the presence of a beam of lithium fluoride. Ultra-high vacuum systems (in the range 10^{-11} mm Hg or better) should be used in conjunction with long clean-up times of the filaments to guard against any impurities masking or upsetting the process of ionization. Such ultra-high vacuum systems are not difficult to build today; in fact, we consistently can obtain 5×10^{-10} mm Hg with a small system using an ion pump and a liquid nitrogen cold trap with the only outgassing done by a hand torch for about one hour. This system is made of stainless steel and uses copper shear gaskets and a teflon seal in the high-vacuum valve.

APPENDIX

REFERENCES

1. K. H. Kingdom and I. Langmuir, Phys. Rev. 21:380 (1923).

2. H. E. Ives, Phys. Rev. 21:385 (1923).

3. N. O. Morgulis, J. Exp. Theo. Phys. (U.S.S.R.) 4:684 (1934).

4. P. P. Sutton and J. E. Mayer, J. Chem. Phys., 3:20 (1935).

5. K. H. Kingdom and I. Langmuir, Proc. Roy. Soc. (London) A107,61 (1925).

6. M. N. Saha, Phil. Mag. 46:534 (1923).

7. M. J. Copley and T. E. Phipps, Phys. Rev. 45:344 (1934).

8. M. J. Copley and T. E. Phipps, Phys. Rev. 48:960 (1935).

9. S. Datz and E. H. Taylor, J. Chem. Phys. 25:389 (1956).

10. L. N. Dobretsov, J. Expt. Theo. Phys. (U.S.S.R.) 17:301 (1947).

11. J. Zemel, J. Chem. Phys., 28:410 (1958).

12. E. Y. Zandberg and N. I. Ionov, Soviet Phys. Uspehki, (U.S.S.R.) 67:255 (1959).

13. Ramsay, Norman F., Molecular Beams, Oxford Press, 1956.

14. L. I. Schiff, Quantum Mechanics, McGraw-Hill, (1955).

15. N. I. Ionov, J. Exptl. Theo. Phys. (U.S.S.R.), 18:174 (1948).

16. S. Datz and E. H. Taylor, J. Chem. Phys., 25:395 (1956).

17. I. Langmuir, Phys. Rev. 2:331 (1913).

18. A. Sommerfeld, Z. Physik, 47:1 (1928).

19. R.L.E. Seifert and T. E. Phipps, Phys. Rev., 56:652 (1939).

20. D. Turnbull and T. E. Phipps, Phys. Rev., 56:663 (1939).

21. Handbook of Chemistry and Physics, 35th edition (1953-1954), Chemical Rubber Publishing Company.

APPENDIX

DERIVATION OF THE SAHA-LANGMUIR EQUATION

The Saha equation relates the concentrations of ions, atoms, and electrons in a gas in thermodynamic equilibrium[6].

$$\frac{n_+ n_-}{n_a} = \left[\frac{2\pi m_e kT}{h^2}\right]^{3/2} \left[\frac{w_+ w_-}{w_a}\right] \exp\left(-\frac{eI}{kT}\right) \qquad \text{(A-1)}$$

where

n_+ = number of positive ions,

n_- = number of electrons,

n_a = number of atoms,

w_+ = statistical weight of ions,

w_- = statistical weight of electrons,

w_a = statistical weight of atoms,

m_e = electron rest mass,

e = electron charge,

h = Plank's constant,

k = Boltzman constant, and

T = Temperature (^oK).

The number of particles striking and leaving (assuming no reflections) one surface of a unit cube in unit

time is related to the number of particles in the cube by

$$n_s = n_t \sqrt{\frac{kT}{2\pi m}}, \tag{A-2}$$

where

n_s = number striking surface per unit time,

n_t = total number of particles in cube.

Sommerfeld's modified Richardson Equation may be written[18]

$$n_{s-} = \frac{2\pi m k^2 T^2 w_-}{h^3} \exp\left(-\frac{e\phi}{kT}\right), \tag{A-3}$$

where

ϕ is the work function of the surface.

Combining Eqs. (A-a) and (A-3), we obtain

$$n_- = n_t = n_{s-} \sqrt{\frac{2\pi m}{kT}} = \left[\frac{2\pi m k T}{h^2}\right]^{3/2} w_- \exp\left(-\frac{e\phi}{kT}\right). \tag{A-4}$$

Substituting (A-4) into (A-1), yields

$$\frac{n_+}{n_a} = \frac{w_+}{w_a} \exp\left[\frac{e(\phi - I)}{kT}\right]. \tag{A-5}$$

Permitting the possibility of reflections to occur, (A-5)

will be modified to

$$\frac{n_+}{n_a} = \frac{1 - r_+}{1 - r_a} \frac{w_+}{w_a} \exp\left[\frac{e(\phi - I)}{kT}\right], \qquad \text{(A-6)}$$

which is generally known as the Saha-Langmuir equation.

ACKNOWLEDGMENT

Grateful acknowledgment is extended to Dr. Frank S. Barnes who in large measure is responsible for the conception and successful completion of this research. I am also indebted to Mr. Max Humpal for the fabrication and machining of various parts. This work was performed under the auspices of the United States Army Signal Supply Agency, Department of the Army Project No. 3A99-15-001.